# GW (oneshot) + DMFT documentation

June 9, 2017

## Contents

# 1 Introduction

This document provides our prescription of the combination of a GW calculation for correlated materials with DMFT applied only to a subset of correlated orbitals. At this level, the GW calculation will be performed only once at the beginning (one-shot) based on a DFT Hamiltonian $H^{DFT}$ to obtain a nonlocal GW Selfenergy $\Sigma^{GW}$ for all states. In addition, the local part of $\Sigma^{GW}$ of a subset of strongly correlated orbitals will be replaced by a Selfenergy $\Sigma^{DMFT}$ obtained within a selfconsistent DMFT scheme, where the selfconsistency is done including the full nonlocal effects of the combined Selfenergy.

No further selfconsistency apart from the DMFT cycle will be performed, *i.e.* no update of $\Sigma^{GW}$ will be done. By this, the final interacting system will be de-

scribed by a Green's function with the non-interacting DFT dispersion, excluding the exchange-correlation potential, corrected by a non-local GW Selfenergy where the non-local components correspond to $\Sigma^{GW} = G_0W_0$, while the local components of the correlated orbitals correspond to $\Sigma^{DMFT}$. This $\Sigma^{DMFT}$ is usually different to the one obtained by a standard DMFT calculation since the selfconsistency is done with the inclusion of the nonlocal parts of the Selfenergy.

Extensions to a full GW+DMFT selfconsistency will come later, but selfconsistency in the effective interaction $U$ is planned.

# 2 Approximation to the free energy functional $\Gamma[G, W]$: Combination of GW and DMFT

As stated by Almbladh[ref], the free energy of a solid can be written in terms of a functional $\Gamma[G, W]$ of the fully dressed Green's function $G$ and the screened Coulomb interaction $W$. While an analytic expression for $\Gamma$ is not known, it can be shown that it can be separated into a Hartree part $\Gamma^H$ and a correction arising from all other many-body effects $\Psi$

$$\Gamma[G, W] = \Gamma^H[G, W] + \Psi[G, W]. \tag{2.1}$$

The many-body correction $\Psi[G, W]$ is the sum of all skeleton diagrams that are irreducible with respect to both one-electron propagator and interaction lines. The Hartree diagram does not fulfill this property so it is not included in this series. It has the properties

$$\frac{\delta\Psi}{\delta G} = \Sigma^{XC} \tag{2.2}$$

$$\frac{\delta\Psi}{\delta W} = -\frac{1}{2}P, \tag{2.3}$$

where $\Sigma^{XC}$ is the exchange-correlation Selfenergy corresponding to the fully dressed Green's function $G$, thus excluding the Hartree part $\Sigma^H$. $P$ is the full polarization of the system that screens the bare Coulomb interaction $V$ down to the screened interaction $W$.

Since the screened interaction $W$ is much smaller than the bare interaction $V$, a perturbative ansatz should converge much faster for $W$ than for $V$ for obtaining the many-body correction $\Psi[G, W]$.

One possibility is the GW approximation, which expands $\Psi[G, W]$ in powers of the screened interaction $W$ and truncates the series at first order. The resulting expression is thus

$$\Psi[G, W] \approx -\frac{1}{2}\mathrm{Tr}(GWG). \tag{2.4}$$

Using equations (2.2) and (2.3), we immediately obtain the $GW$ Selfenergy and polarization as

$$\Sigma^{GW} = -GW \tag{2.5}$$

$$P^{GW} = GG. \tag{2.6}$$

Please note that this expression is correct for working on the imaginary time or frequency axis. On the real time or frequency axis the prefactor for $\Sigma^{GW}$ is $i$ instead of $-1$. For $P$ I need to check...

While this approximation goes beyond the level of a static Hartree-Fock approximation, it is only an expansion up to first order in $W$ and thus justified only when $W$ is small, i.e. in case of weakly correlated systems. Thus, it is tempting to combine $GW$ with other methods like DMFT for an improved treatment of correlated systems.

In the GW+DMFT scheme, we first separate the $\Psi$ functional into its local and nonlocal parts

$$\Psi[G,W] = \Psi_{\text{nonloc}}[G,W] + \Psi_{\text{loc}}[G,W], \tag{2.7}$$

Is this probably not exact where usually the nonlocal part is approximated by $GW$, while the local part is usually approximated by DMFT, but right now we do not want to decide on a specific method and only focus on how to separate the local and nonlocal contributions.

We only want to impose one specific condition: First, we work in an orbital separated scheme, where we separate the full Hilbert space $L + H$ into a correlated subspace $L$ and the remaining subspace $H$. Then, our defintion of $\Psi_{\text{loc}}$ is the following: $\Psi_{\text{loc}}$ is generated only from the local components of $G$ and $W$ in the correlated subspace, i.e.

$$\Psi[G,W] = \Psi_{\text{nonloc}}[G,W] + \underbrace{\Psi[G^{\text{loc},L}, W^{\text{loc},L}]}_{\Psi_{\text{loc}}}. \tag{2.8}$$

By this, all internal processes contributing to $\Psi_{\text{loc}}$ are restricted to the smaller correlated subspace $L$ and its local $G$ and $W$. This construction already points to the usage of DMFT for $\Psi_{\text{loc}}$, but it is instructive not to fix on a specific method yet. All other contributions to the full $\Psi$ are now defined to be originating from $\Psi_{\text{nonloc}}[G,W]$. We now have to explain what we actually mean by the two objects $\Psi_{\text{nonloc}}$ and $\Psi_{\text{loc}}$.

First, let us start with the nonlocal part $\Psi_{\text{nonloc}}$. Rewriting Eq. (2.8) in the following way naturally leads us to its definition via

$$\begin{aligned} \Psi[G,W] &= \Psi_{\text{nonloc}}[G,W] + \Psi[G^{\text{loc},L}, W^{\text{loc},L}] && (2.9)\\ &= \underbrace{\Psi[G,W] - \Psi[G^{\text{loc},L}, W^{\text{loc},L}]}_{:=\Psi_{\text{nonloc}}} + \Psi[G^{\text{loc},L}, W^{\text{loc},L}]. && (2.10) \end{aligned}$$

By this, we immediately see that applying any approximation $A$ to $\Psi_{\text{nonloc}}$ and $\Psi_{\text{loc}}$ will give us the approximate functional $\Psi^A = \Psi^A_{\text{nonloc}} + \Psi^A_{\text{loc}}$.

Side remark: Using the same approximation on both terms will not create any doublecounting or loss of terms, regardless of whether we use an orbital separated scheme or not.

It starts to get really interesting when we use two different approximations $A$ and $B$ to treat the two terms

$$\Psi[G,W] \approx \Psi^{A}_{\text{nonloc}}[G,W] + \Psi^{B}_{\text{loc}}[G^{\text{loc},L}, W^{\text{loc},L}]. \tag{2.11}$$

The main point here is IS THERE REALLY NO OVERLAP/DOUBLECOUNTING IN THIS SCHEME?

In the context of GW+DMFT we will now approximate the nonlocal part by GW and the local part by DMFT. The GW approximation is usually performed as a single-shot, and thus based on the DFT Green's function $G^0$ and RPA screened interaction $W^0$, while the local functional from DMFT is obtained from the impurity Green's function and interaction, i.e.

$$\Psi[G,W] \approx \Psi^{GW}_{\text{nonloc}}[G,W] + \Psi^{DMFT}_{\text{loc}}[G^{\text{loc},L}, W^{\text{loc},L}] \tag{2.12}$$

$$= -\frac{1}{2}\Big(G^0W^0G^0 - G^{0,\text{loc},L}W^{0,\text{loc},L}G^{0,\text{loc},L}\Big) + \Psi^{DMFT}[G^{\text{imp},L}, W^{\text{imp},L}]. \tag{2.13}$$

Please note that in the orbital separated scheme

$$\Sigma^{GW,\text{loc},L} \neq \sum_k \frac{\delta}{\delta G^L_k}\Big(-\frac{1}{2}G^{0,\text{loc},L}W^{0,\text{loc},L}G^{0,\text{loc},L}\Big), \tag{2.14}$$

but this is not relevant here. Using equations (2.2) and (2.3) we obtain for the GW+DMFT Selfenergy and polarization

$$\Sigma_{ab} = \begin{cases} -[G^0W^0]_{ab} + [G^{0,\text{loc},L}W^{0,\text{loc},L}]_{ab} + \Sigma^{\text{imp},XC,L}_{ab} & \text{for } a,b \in L \\ -[G^0W^0]_{ab} & \text{for } a \text{ or/and } b \in H \end{cases} \tag{2.15}$$

$$P_{abcd} = \begin{cases} [G^0G^0]_{abcd} - [G^{0,\text{loc},L}G^{0,\text{loc},L}]_{abcd} + P^{\text{imp},L}_{abcd} & \text{for } a,b,c,d \in L \\ [G^0G^0]_{abcd} & \text{for } \{a,b,c,d\} \cap H \neq \emptyset \end{cases} \tag{2.16}$$

Limiting cases:

$W$ **small:** In this case the Selfenergy will be well described already by GW, so the impurity solution will basically give the same result $G^{0,\text{loc},L}W^{0,\text{loc},L} = \Sigma^{\text{imp},L}$. The two terms cancel and we fully regain the GW result. NO doublecounting like in FLL LDA+U or LDA+DMFT!

**W large:** Then the GW Selfenergy contribution within the subspace $L$ is basically given by the impurity solution. There is no mismatch of exchange terms originating from outside the space $L$, since only the local impurity exchange is removed from GW and replaced by the local impurity DMFT exchange. But this term can be different due to rearrangements of the local impurity charge. This contribution is not yet considered in the GW screening since no GW selfconsistency has been applied. Can we now do another GW calculation only

replacing the new contribution from the impurity states? Then we perform a GW selfconsistency including the local vertex corrections from DMFT, in similar spirit as Boehnke et al., but additionally with improved transitions between $L$ and $H$ which they do not update.

The 2-particle selfconsistency cycle over $W$ is not conserving! In what way does this affect the spectra? Other two-particle quantities? Hartmut said something like Plasmons cannot be properly treated due to the nonconserving properties.

# 3 The GW+DMFT Doublecounting

In the section above we discussed that the "doublecounting" factor that has to be subtracted from the GW Selfenergy and Polarization should be

$$\Sigma^{GW,DC} = -G^{0,\mathrm{loc},L} W^{0,\mathrm{loc},L} \tag{3.1}$$

$$P^{GW,DC} = G^{0,\mathrm{loc},L} G^{0,\mathrm{loc},L} \tag{3.2}$$

This method using $\Sigma^{GW,DC} = -G^{0,\mathrm{loc},L} W^{0,\mathrm{loc},L}$ can be understood as calculating a GW Selfenergy excluding any contributions arising exclusively in the correlated subspace, and then adding the contributions arising only in the correlated subspace via DMFT.

Other choices have been discussed, for example what we have been using for now is to subtract all local terms from GW

$$\Sigma^{GW,DC^*} = -[G^0 W^0]^{\mathrm{loc},L} = \frac{1}{N_k} \sum_k \Sigma^{GW,L} \tag{3.3}$$

$$P^{GW,DC^*} = [G^0 G^0]^{\mathrm{loc},L} = \frac{1}{N_k} \sum_k P^{GW,L} \tag{3.4}$$

IMPORTANT: These two doublecounting factors are not equal as long as we restrict to a smaller subspace $L$, since the local component of the Selfenergy and Polarization contain terms arising from the interaction with the smaller subspace $L$ and the remaining part $R = H \setminus L$

$$\Sigma^{GW,loc} = -G^{0,\mathrm{loc}}_{LL} W^{0,\mathrm{loc}}_{LL} - G^{0,\mathrm{loc}}_{RR} W^{0,\mathrm{loc}}_{LRRL} \tag{3.5}$$

Only when $L = H$ is the full Hilbert space, they are equal since the second term is also included. This problem does not arise for the polarization, since there is no four-index object like $W$ which couples the two spaces.

In Fig.1 we show a comparison between the Selfenergy $\Sigma(i\omega_n)$ obtained from a $G_0W_0$ (7x7x7 k-points) calculation, and GW+DMFT using the $G_0W_0$ input for a $t_{2g}$-only model for $SrVO_3$ with $U(\omega)$ interaction determined from cRPA. The GW-local is the k-averaged part of the GW Selfenergy, and the GW+DMFT Selfenergy is the local Selfenergy of the impurity model after convergence of the GW+DMFT cycle including the non-local components of the GW Selfenergy but subtracting the GW-local part as the doublecounting. This means we have thrown away all contributions $G^{0,\mathrm{loc}}_{RR} W^{0,\mathrm{loc}}_{LRRL}$ arising from the interaction between the correlated subspace and the rest.

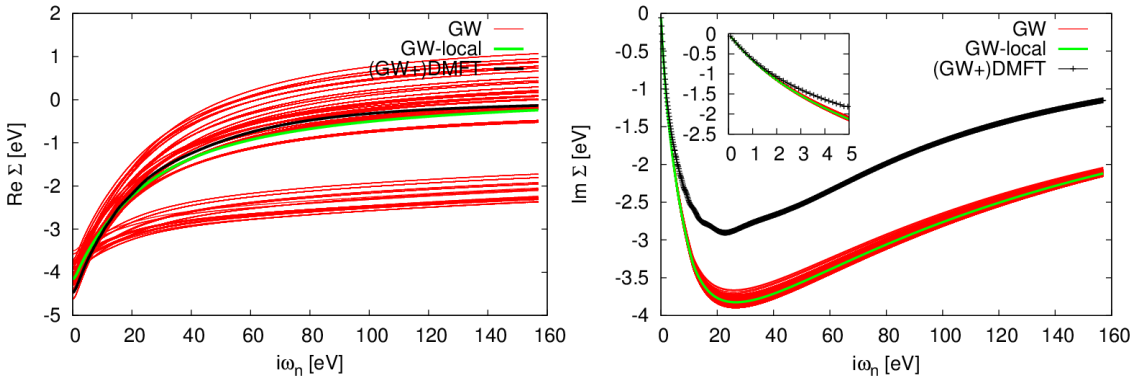


Figure 1: The Selfenergy $\Sigma(i\omega_n)$ obtained from $G_0W_0$ (7x7x7 k-points) and GW+DMFT using the $G_0W_0$ input for a $t_{2g}$-only model for $SrVO_3$ with $U(\omega)$ interaction determined from cRPA. As the doublecounting $\Sigma^{DC}_{GW}$ the local part of the GW Selfenergy $\sum_k GW$ on the correlated orbitals been subtracted (green line, called GW-local). One clearly sees a mismatch between this term and the DMFT Selfenergy (black line), which is due to the terms contributing to the local Selfenergy that arise from the coupling between the subspace and the remaining states and also the nonlocal contributions to the local part which cannot be captured by DMFT.

The discrepancy between the impurity Selfenergy and the k-averaged GW Selfenergy, that can be seen especially in the imaginary part, can then in principle have to reasons:

One contribution will be the contributions from the subspace with the rest $G^{0,\mathrm{loc}}_{RR}W^{0,\mathrm{loc}}_{LRRL}$, as already discussed. Another contribution can arise from the cRPA screening to obtain the effective interaction $U(\omega)$. If the bare value is not the proper one, this would also lead to a discrepancy especially in the tail sections of the Selfenergy, i.e. if the value is too small, the tail will be smaller.

**PLEASE NOTE:** The GW doublecounting factor $\Sigma^{GW,DC}$ should not contain the Hartree part, since the GW Selfenergy $\Sigma^{GW}_{XC}$ does not contain it.

First tests using both methods in SrVO3 show that $-G^{0,\mathrm{loc},L}W^{0,\mathrm{loc},L}$ seems to reduce the rernormalization in the unoccupied part. With the other DC there seemed to be a shift in the chemical potential where the bands are slightly too low, but the reason for this is not fully clear and maybe something else might be responsible, but I don't think so.

## 3.1 Possible problems with the DC

One important factor is the causality of the different DC schemes. The GW Selfenergy is causal and the impurity Selfenergy is causal, but subtracting a DC term can make the combined Selfenergy noncausal

$$\Sigma^{GW+DMFT} = \Sigma^{GW,loc} - \Sigma^{DC} + \Sigma^{imp}. \tag{3.6}$$

It only comes down to personal preference, whether the DC should be understood as taking out contibutions from GW, so that GW is a correction to DMFT

$$\Sigma^{GW+DMFT} = \Sigma^{imp} + \left(\Sigma^{GW,loc} - \Sigma^{DC}\right), \tag{3.7}$$

or whether one takes out contibutions from DMFT, so that DMFT is a correction to GW

$$\Sigma^{GW+DMFT} = \Sigma^{GW,loc} + \left(\Sigma^{imp} - \Sigma^{DC}\right). \tag{3.8}$$

## 3.2 Evaluating the doublecounting factor $\Sigma^{DC}_{GW} = G_{loc}W_{loc}$

When evaluating the doublecounting factor

$$\Sigma^{DC}_{GW} = -[G^{\mathrm{loc}}W^{\mathrm{loc}}], \tag{3.9}$$

we want to construct a Selfenergy which is solution of the DMFT impurity problem within the GW approximation. By this, we regain exactly the full GW solution if we "use GW as the impurity solver". In the GW+DMFT approach we use instead DMFT as the impurity solver, which should give us corrections that go beyond the GW approximation on the impurity.

Since we usually use the $G_0W_0$ approximation in the continuum, for consistency we also have to solve the impurity problem within $G_0W_0$, otherwise we would not regain the full $G_0W_0$ solution, as just discussed. This means $G^{\mathrm{loc}}$ is the local DFT Green's function in the correlated subspace and $W^{\mathrm{loc}}$ is the local *effective* fully screened interaction on the impurity. $W^{\mathrm{loc}}$ is just related to the effective "bare" interaction that is the input for DMFT via the Dyson equation

$$\mathcal{U}^{-1} = [W^{loc}]^{-1} + P^{imp}. \tag{3.10}$$

$W^{\mathrm{loc}}$ thus contains all the screening processes but is projected onto the correlated subspace.

To derive the expression for $G^{loc}W^{loc}$ we start with the definitions from the original paper by Hedin (we set $\hbar = 1$). For real time in the continuum the Green's function and the bare Coulomb potential is defined as

$$G(1,2) = -i\langle T\psi(1)\psi^{\dagger}(2)\rangle \tag{3.11}$$

$$V_C(1,2) = \frac{\delta(t_1 - t_2)}{|r_1 - r_2|}, \tag{3.12}$$

where the arguments denote the combined space,spin and time dependence

$$(1) = (r_1, \sigma_1, t_1). \tag{3.13}$$

The Selfenergy in the GW approximation is then given as

$$\Sigma(1,2) = iG(1,2)W(1^+,2), \tag{3.14}$$

where

$$(1^+) = (r_1, \sigma_1, t_1 + \Delta), \quad \Delta \to 0^+. \tag{3.15}$$

It is instructive to investigate the case of no screening when $W$ is equal to the bare Coulomb potential

$$\Sigma(1,2) = iG(1,2)W(1^+,2) \tag{3.16}$$
$$= iG(1,2)\frac{\delta(t_1+\Delta-t_2)}{|r_1-r_2|} \tag{3.17}$$
$$= iG(r_1,\sigma_1,t_1;r_2,\sigma_2,t_1+\Delta)\frac{\delta(t_1+\Delta-t_2)}{|r_1-r_2|} \tag{3.18}$$
$$= \langle T\psi_{\sigma_1}(r_1,t_1)\psi^\dagger_{\sigma_2}(r_2,t_1+\Delta)\rangle\frac{\delta(t_1+\Delta-t_2)}{|r_1-r_2|} \tag{3.19}$$
$$= -\langle\psi^\dagger_{\sigma_2}(r_2)\psi_{\sigma_1}(r_1)\rangle\frac{\delta(t_1+\Delta-t_2)}{|r_1-r_2|} \tag{3.20}$$
$$\Rightarrow \Sigma(r_1,\sigma_1,t_1;r_2,\sigma_2,t_2) = -\frac{\langle\psi^\dagger_{\sigma_2}(r_2)\psi_{\sigma_1}(r_1)\rangle}{|r_1-r_2|}\delta(t_1-t_2). \tag{3.21}$$

In this case the GW is just the bare Fock-exchange! There is no Hartree contribution in the GW Selfenergy. This means GW is basically just dynamically screened exchange? Where do correlation terms come in?

Since we work on the Matsubara axis, we rewrite the equation for imaginary times

$$G(1,2) = -\langle T_\tau\psi(1)\psi^\dagger(2)\rangle \tag{3.22}$$
$$\Sigma(1,2) = -G(1,2)W(1^+,2), \tag{3.23}$$

where the arguments now denote the imaginary time argument

$$(1) = (r_1,\sigma_1,\tau_1) \tag{3.24}$$
$$(1^+) = (r_1,\sigma_1,\tau_1+\Delta). \tag{3.25}$$

For consistency we can check that setting $W$ equal the bare Coulomb interaction indeed reduces to the Fock-exchange with the correct sign. $GV_C$ is positive but again exchaning the operators leads to an overall minus sign, so the total contribution indeed is negative and identical to the result on the real-time axis.

Introducing a local basis $\langle r|\chi^\sigma_m\rangle = \chi^\sigma_m(r)$ we can obtain the matrix elements of the Selfenergy in this basis

$$\langle m_1\sigma_1|\Sigma(\tau_1,\tau_2)|m_2\sigma_2\rangle = \langle\chi^{\sigma_1}_{m_1}|\Sigma(\tau_1,\tau_2)|\chi^{\sigma_2}_{m_2}\rangle \tag{3.26}$$
$$= -\int\int dr_1dr_2\ \chi^{\sigma_1*}_{m_1}(r_1)G(r_1,\sigma_1,\tau_1;r_2,\sigma_2,\tau_2) \tag{3.27}$$
$$\times W(r_1,\tau_1+\Delta;r_2,\tau_2)\chi^{\sigma_2}_{m_2}(r_2) \tag{3.28}$$

Expanding the Green's function in this local basis as

$$G(r_1,\sigma_1,\tau_1;r_2,\sigma_2,\tau_2) = \sum_{kl}\chi^{\sigma_1}_k(r_1)G^{\sigma_1\sigma_2}_{kl}(\tau_1,\tau_2)\chi^{\sigma_2*}_l(r_2) \tag{3.29}$$

we get

$$\langle m_1\sigma_1|\Sigma(\tau_1,\tau_2)|m_2\sigma_2\rangle = -\sum_{kl}\int\int dr_1dr_2\ G^{\sigma_1\sigma_2}_{kl}(\tau_1,\tau_2) \tag{3.30}$$
$$\times\chi^{\sigma_1*}_{m_1}(r_1)\chi^{\sigma_2*}_l(r_2)W(r_1,\tau_1+\Delta;r_2,\tau_2)\chi^{\sigma_1}_k(r_1)\chi^{\sigma_2}_{m_2}(r_2) \tag{3.31}$$

The last term we identify as the matrix element of the fully screened interaction

$$\langle m_1 l|W(\tau_1+\Delta,\tau_2)|km_2\rangle = \int\int dr_1 dr_2 \chi^{\sigma_1 *}_{m_1}(r_1)\chi^{\sigma_2 *}_{l}(r_2)W(r_1,\tau_1+\Delta;r_2,\tau_2)\chi^{\sigma_1}_{k}(r_1)\chi^{\sigma_2}_{m_2}(r_2) \tag{3.32}$$

With this we finally get the expression

$$\langle m_1\sigma_1|\Sigma(\tau_1,\tau_2)|m_2\sigma_2\rangle = -\sum_{kl}\langle m_1 l|W(\tau_1+\Delta,\tau_2)|km_2\rangle\, G^{\sigma_1\sigma_2}_{kl}(\tau_1,\tau_2) \tag{3.33}$$

We can simplify this expression by assuming time translational invariance and assume the local Green's function to be orbital- and spin-diagonal

$$\Sigma^{\sigma}_{m}(\tau) = -\sum_{k}\langle mk|W(\tau+\Delta)|km\rangle\, G^{\sigma}_{k}(\tau) \tag{3.34}$$

Again we see that the GW Selfenergy is basically dynamical screened exchange.

Applying the Fourier transform and inserting the Fourier transform of $G(ix_n)$ and $W(i\nu_n)$ we get for the Selfenergy on the Matsubara axis

$$\Sigma^{\sigma}_{m}(i\omega_n) = -\sum_{k}\int_0^\beta d\tau\ \left[\frac{1}{\beta}\sum_i \langle mk|W(i\nu_i)|km\rangle\, \mathrm{e}^{-i\nu_i(\tau+\Delta)}\right]\left[\frac{1}{\beta}\sum_j G^{\sigma}_{k}(ix_j)\mathrm{e}^{-i\nu_i\tau}\right]\mathrm{e}^{i\omega_n\tau} \tag{3.35}$$

$$= -\sum_{k}\sum_{ij}\langle mk|W(i\nu_i)|km\rangle\, G^{\sigma}_{k}(ix_j)\int_0^\beta d\tau\ \frac{1}{\beta^2}\mathrm{e}^{i(\omega_n-\nu_i-x_j)\tau}\mathrm{e}^{-i\nu_i\Delta} \tag{3.36}$$

$$= -\frac{1}{\beta}\sum_{k}\sum_{j}\langle mk|W(i\nu_j)|km\rangle\, G^{\sigma}_{k}(i\omega_n-i\nu_j)\mathrm{e}^{-i\nu_j\Delta} \tag{3.37}$$

(This form should not be used, see below) Or rewriting the frequency sum we get the alternative version

$$\Sigma^{\sigma}_{m}(i\omega_n) = -\frac{1}{\beta}\sum_{k}\sum_{j}\langle mk|W(i\omega_n-ix_j)|km\rangle\, G^{\sigma}_{k}(ix_j)\mathrm{e}^{-i(\omega_n-x_j)\Delta} \tag{3.38}$$

$$= -\frac{1}{\beta}\sum_{k}\sum_{j}\langle mk|W(i\omega_n-ix_j)|km\rangle\, G^{\sigma}_{k}(ix_j)\mathrm{e}^{ix_j\Delta} \tag{3.39}$$

The last factor $\mathrm{e}^{ix_j\Delta}$ is important to ensure convergence of the frequency sum. This form is actually much better for practical implementation because the slow $1/i\omega_j$ convergence does not include a shift which slowes down the convergence even more. Since $\Delta\to 0^+$ we can directly see that we regain the correct Fock-exchange when replacing $W$ by the constant bare Coulomb interaction! For the GW solution of the impurity model the sum over the orbital indices $k$ is performed only over the correlated subspace which spans the Hilbert space of the Anderson impurity model.

It is instructive to look at the case of a simple degenerate $t_{2g}$-only model like for $SrVO_3$. In this case we define the screened on-site Coulomb matrix element and the screened Hund's exchange as

$$\langle kk|W(i\nu)|kk\rangle = U_0(i\nu) \tag{3.40}$$

$$\langle mk|W(i\nu)|km\rangle = J(i\nu), \quad k\neq m. \tag{3.41}$$

With this we get the explicit expression for the $t_{2g}$ Selfenergy

$$\Sigma^{\sigma}(i\omega_n) = -\frac{1}{\beta}\sum_{ix_j}\Big(U_0(i\omega_n - ix_j) + 2J(i\omega_n - ix_j)\Big)G^{\sigma}(ix_j)\mathrm{e}^{ix_j\Delta} \tag{3.42}$$

The first term corresponding to $U_0$ is similar to a dynamical self-interaction correction since it originates from an interaction with a state with the same orbital and spin index. The second term corresponding to $J$ is a dynamical intraatomic exchange contribution since it originates from an interaction with a state in a different orbital and with the same spin index.

Again we see that the GW Selfenergy has the characteristics of a dynamically screened Fock-exchange term.

## 3.3 High-frequency correction for GW-DC version1

This should not be used because this form converges slower When evaluating the frequency sum for the doublecounting in the form

$$\Sigma^{\sigma}_m(i\omega_n) = -\frac{1}{\beta}\sum_k\sum_j \langle mk|W(i\nu_j)|km\rangle\, G^{\sigma}_k(i\omega_n - i\nu_j)\mathrm{e}^{-i\nu_j\Delta} \tag{3.43}$$

the convergence is not so good and needs to be corrected for the high-frequency parts. We use a high-frequency form to fit the Green's function and interaction given by

$$W(i\nu_n) \approx w_0 + \frac{w_2}{(i\nu_n)^2} \quad \in \mathbb{R} \tag{3.44}$$

$$G(i\omega_n) \approx \frac{1}{i\omega_n} + \frac{g_2}{(i\omega_n)^2} \tag{3.45}$$

We need to evaluate the following high-frequency terms (orbital/spin etc indices are suppressed)

$$-\frac{1}{\beta}\sum_{j\neq 0}\left(w_0 + \frac{w_2}{(i\nu_j)^2}\right)\left(\frac{1}{i\omega_n - i\nu_j} + \frac{g_2}{(i\omega_n - i\nu_j)^2}\right)\mathrm{e}^{-i\nu_j\Delta} \tag{3.46}$$

$$= -\frac{1}{\beta}\sum_{j\neq 0}\left(\frac{w_0}{i\omega_n - i\nu_j} + \frac{w_0 g_2}{(i\omega_n - i\nu_j)^2} + \frac{w_2}{(i\nu_j)^2(i\omega_n - i\nu_j)} + \frac{w_2 g_2}{(i\nu_j)^2(i\omega_n - i\nu_j)^2}\right)\mathrm{e}^{-i\nu_j\Delta}. \tag{3.47}$$

Evaluating the terms analytically we get for the first term (compare Steffen's PhD

thesis for the derivation)

$$-\frac{1}{\beta}\sum_{j\neq 0}\frac{w_0}{i\omega_n - i\nu_j}\mathrm{e}^{-i\nu_j\Delta} = -\frac{w_0}{\beta}\left(-\frac{1}{i\omega_n - 0}\mathrm{e}^{-i0\Delta} + \sum_j \frac{1}{i\omega'_j}\mathrm{e}^{-(i\omega_n - i\omega'_j)\Delta}\right) \tag{3.48}$$

$$= -\frac{w_0}{\beta}\left(-\frac{1}{i\omega_n} + \mathrm{e}^{-i\omega_n\Delta}\sum_{j\neq 0}\frac{1}{i\omega'_j}\mathrm{e}^{i\omega'_j\Delta}\right) \tag{3.49}$$

$$= -\frac{w_0}{\beta}\left(-\frac{1}{i\omega_n} + \frac{\beta}{2}\right) \tag{3.50}$$

$$= w_0\left(\frac{1}{i(2n+1)\pi} - \frac{1}{2}\right). \tag{3.51}$$

The second term

$$-\frac{1}{\beta}\sum_{j\neq 0}\frac{w_0 g_2}{(i\omega_n - i\nu_j)^2}\mathrm{e}^{-i\nu_j\Delta} = -\frac{w_0 g_2}{\beta}\sum_{j\neq 0}\frac{1}{(i\omega'_j)^2}\mathrm{e}^{-(i\omega_n - i\omega'_j)\Delta} \tag{3.52}$$

$$= -\frac{w_0 g_2}{\beta}\mathrm{e}^{-i\omega_n\Delta}\sum_{j\neq 0}\frac{1}{(i\omega'_j)^2}\mathrm{e}^{i\omega'_j\Delta} \tag{3.53}$$

$$= -\frac{w_0 g_2}{\beta}\mathrm{e}^{-i\omega_n\Delta}\left(-\frac{1}{(i\omega'_{j=0})^2}\mathrm{e}^{i\omega'_{j=0}\Delta} + \sum_j \frac{1}{(i\omega'_j)^2}\mathrm{e}^{i\omega'_j\Delta}\right) \tag{3.54}$$

$$= -\frac{w_0 g_2}{\beta}\mathrm{e}^{-i\omega_n\Delta}\left(\frac{\beta^2}{\pi^2} + \frac{-2\Delta - \beta}{4}\beta\right) \tag{3.55}$$

$$= w_0 g_2\beta\left(\frac{1}{4} - \frac{1}{\pi^2}\right). \tag{3.56}$$

The third term

$$-\frac{1}{\beta}\sum_{j\neq 0}\frac{w_2}{(i\nu_j)^2(i\omega_n - i\nu_j)}\mathrm{e}^{-i\nu_j\Delta} \tag{3.57}$$

$$= -\frac{iw_2\beta^2}{(8n-4)\pi^3}\left(\frac{2n-1}{2n+1}\frac{\pi^2}{6}\right) - \frac{iw_2\beta^2}{(8n+12)\pi^3}\left(\frac{2n+3}{2n+1}\frac{\pi^2}{6} - \frac{8n+12}{(2n+1)^3}\right) \tag{3.58}$$

$$= -\frac{iw_2\beta^2}{\pi^3}\left(\frac{\pi^2}{12(2n+1)} - \frac{1}{(2n+1)^3}\right) \tag{3.59}$$

$$= -\frac{iw_2\beta^2}{(2n+1)\pi^3}\left(\frac{\pi^2}{12} - \frac{1}{(2n+1)^2}\right). \tag{3.60}$$

The fourth term

$$-\frac{1}{\beta}\sum_{j\neq 0}\frac{w_2 g_2}{(i\nu_j)^2(i\omega_n - i\nu_j)^2}\mathrm{e}^{-i\nu_j\Delta} \tag{3.61}$$

$$= -\frac{w_2 g_2 \beta^3}{4\pi^4(2n-1)^2}\left(\frac{(2n-1)^2}{(2n+1)^2}\frac{\pi^2}{6}\right) - \frac{w_2 g_2\beta^3}{4\pi^4(2n+3)^2}\left(\frac{(2n+3)^2}{(2n+1)^2}\frac{\pi^2}{6} - 12\frac{(2n+3)^2}{(2n+1)^4}\right) \tag{3.62}$$

$$= -\frac{w_2 g_2\beta^3}{4\pi^4}\left(\frac{\pi^2}{3(2n+1)^2} - \frac{12}{(2n+1)^4}\right) \tag{3.63}$$

$$= -\frac{w_2 g_2\beta^3}{\pi^4(2n+1)^2}\left(\frac{\pi^2}{12} - \frac{3}{(2n+1)^2}\right). \tag{3.64}$$

## 3.4 High-frequency correction for GW-DC version2

When evaluating the frequency sum for the doublecounting in the form

$$\Sigma^\sigma_m(i\omega_n) = -\frac{1}{\beta}\sum_k\sum_j \langle mk|W(i\omega_n - ix_j)|km\rangle\, G^\sigma_k(ix_j)\mathrm{e}^{ix_j\Delta} \tag{3.65}$$

the convergence is quite fast but still needs to be corrected for the high-frequency parts. We use a high-frequency form to fit the Green's function and interaction given by

$$W(i\nu_n) \approx w_0 + \frac{w_2}{(i\nu_n)^2} \ \in \mathbb{R} \tag{3.66}$$

$$G(i\omega_n) \approx \frac{1}{i\omega_n} + \frac{g_2}{(i\omega_n)^2} \tag{3.67}$$

We need to evaluate the following high-frequency terms (orbital/spin etc indices are suppressed, and the $j = n$ term is taken out because the form of $W$ diverges at this point)

$$-\frac{1}{\beta}\sum_{j\neq n}\left(w_0 + \frac{w_2}{(i\omega_n - ix_j)^2}\right)\left(\frac{1}{ix_j} + \frac{g_2}{(ix_j)^2}\right)\mathrm{e}^{ix_j\Delta} \tag{3.68}$$

$$= -\frac{1}{\beta}\sum_{j\neq n}\left(\frac{w_0}{ix_j} + \frac{w_0 g_2}{(ix_j)^2} + \frac{w_2}{ix_j(i\omega_n - ix_j)^2} + \frac{w_2 g_2}{(ix_j)^2(i\omega_n - ix_j)^2}\right)\mathrm{e}^{ix_j\Delta}. \tag{3.69}$$

Evaluating the terms analytically we get for the first term (compare Steffen's PhD thesis for the derivation)

$$-\frac{1}{\beta}\sum_{j\neq n}\frac{w_0}{ix_j}\mathrm{e}^{ix_j\Delta} = -\frac{w_0}{\beta}\left(-\frac{1}{ix_n}\mathrm{e}^{ix_n\Delta} + \sum_j \frac{1}{ix_j}\mathrm{e}^{ix_j\Delta}\right) \tag{3.70}$$

$$= w_0\left(\frac{1}{i(2n+1)\pi} - \frac{1}{2}\right). \tag{3.71}$$

The second term

$$-\frac{1}{\beta}\sum_{j\neq n}\frac{w_0 g_2}{(ix_j)^2}\mathrm{e}^{ix_j\Delta} = -\frac{w_0 g_2}{\beta}\left(-\frac{1}{(ix_n)^2}\mathrm{e}^{ix_n\Delta}+\sum_j\frac{1}{(ix_j)^2}\mathrm{e}^{ix_j\Delta}\right) \tag{3.72}$$

$$= -w_0 g_2\left(\frac{\beta}{(2n+1)^2\pi^2}+\frac{-2\Delta-\beta}{4}\right) \tag{3.73}$$

$$= w_0 g_2\beta\left(\frac{1}{4}-\frac{1}{(2n+1)^2\pi^2}\right). \tag{3.74}$$

The third term (using Maple software)

$$-\frac{1}{\beta}\sum_{j\neq n}\frac{w_2}{ix_j(i\omega_n-ix_j)^2}\mathrm{e}^{ix_j\Delta} = i\frac{w_2\beta^2}{\pi^3}\left(\frac{1}{(2n+1)^3}-\frac{\pi^2}{12(2n+1)}\right) \tag{3.75}$$

$$= i\frac{w_2\beta^2}{(2n+1)\pi^3}\left(\frac{1}{(2n+1)^2}-\frac{\pi^2}{12}\right) \tag{3.76}$$

The fourth term (using Maple software)

$$-\frac{1}{\beta}\sum_{j\neq n}\frac{w_2 g_2}{(ix_j)^2(i\omega_n-ix_j)^2}\mathrm{e}^{ix_j\Delta} = \frac{w_2 g_2\beta^3}{4\pi^4}\left(\frac{12}{(2n+1)^4}-\frac{\pi^2}{3(2n+1)^2}-\frac{\pi^2}{(2n+1)^2}\right) \tag{3.77}$$

$$= \frac{w_2 g_2\beta^3}{(2n+1)^2\pi^4}\left(\frac{3}{(2n+1)^2}-\frac{\pi^2}{3}\right). \tag{3.78}$$

With this, the final expression implemented in the Code is then given by

$$\begin{aligned}\Sigma^\sigma_m(i\omega_n) = \sum_k \Bigg[ &-\frac{1}{\beta}\langle mk|W(0)|km\rangle\, G^\sigma_k(i\omega_n)\\ &-\frac{1}{\beta}\sum_{j\neq n}^{\pm N_{max}}\Big[\langle mk|W(i\omega_n-ix_j)|km\rangle\, G^\sigma_k(ix_j)\\ &\qquad-\langle mk|\left(w_0+\frac{w_2}{(i\omega_n-ix_j)^2}\right)|km\rangle\left(\frac{1}{ix_j}+\frac{g_2}{(ix_j)^2}\right)\Big]\\ &+w_0\left(\frac{1}{i(2n+1)\pi}-\frac{1}{2}\right)+w_0 g_2\beta\left(\frac{1}{4}-\frac{1}{(2n+1)^2\pi^2}\right)\\ &+i\frac{w_2\beta^2}{(2n+1)\pi^3}\left(\frac{1}{(2n+1)^2}-\frac{\pi^2}{12}\right)+\frac{w_2 g_2\beta^3}{(2n+1)^2\pi^4}\left(\frac{3}{(2n+1)^2}-\frac{\pi^2}{3}\right)\Bigg].\end{aligned} \tag{3.79}$$

## 3.5 Doublecounting of the Hartree Term

In the GW+DMFT cycle we have to deal with two types of doublecounting when adding the GW and the DMFT Selfenergy to the Green's function, as partially discussed before

$$\begin{aligned}G(k,i\omega_n) = \big[&\mathbb{1}(i\omega_n+\mu)-H^{DFT}(k)+v^{XC}(k)+\Sigma^{Hartree}_{DFT}\\ &-\Sigma^{XC}_{GW}(k,i\omega_n)+\Sigma^{DC}_{GW}(i\omega_n)-\Sigma_{imp}(i\omega_n)\big]^{-1},\end{aligned} \tag{3.80}$$

The first one is the doublecounting of the Hartree term, which arises since it is taken into account in the DFT and in the DMFT energies resp. Selfenergy. Since DMFT can induce a charge transfer, we will subtract the initial DFT Hartree contribution from the DFT energies, and add the full DMFT Selfenergy which contains a selfconsistent Hartree calculated from the new orbital occupations.

The second one is the local part of the Selfenergy, which is contained in both the GW and the DMFT Selfenergy. Since we assume that DMFT does a better job for the local Selfenergy, we subtract this part from the GW Selfenergy and replace it by the local DMFT Selfenergy. The form of the Hartree part will be derived in section 4. If there is no charge transfer, the Hartree part in the DMFT impurity Selfenergy is identical to the DFT Hartree part, so what has to be subtracted is a Hartree Selfenergy given by the DFT fillings. The fillings are calculated from the DFT Green's function, so in the same sense as the GW doublecounting, we calculate the Hartree solution of the impurity model, and subtract it as a doublecounting. Therefore, it depends on the local DFT Green's function and the effective screened interaction $U(\omega)$.

As derived above in section 3.2, the GW doublecounting $\Sigma^{DC}_{GW}$ does not contain the Hartree but only the exchange part, regardless whether it is calculated as $G_{loc}W_{loc}$ or $[GW]_{loc}$. Therefore, there is no doublecounting of any Hartree term.

We do not need to worry about any exchange doublecounting because in

$$H^{DFT}(k) - v^{XC}(k) \tag{3.81}$$

there is only the Hartree contribution left. In the full combination of

$$\underbrace{H^{DFT}(k) - v^{XC}(k) - \Sigma^{Hartree}_{DFT}}_{\text{no exchange}} + \underbrace{\Sigma^{XC}_{GW}(k, i\omega_n) - \Sigma^{DC}_{GW}(i\omega_n)}_{\text{only nonlocal exch.}} + \underbrace{\Sigma_{imp}(i\omega_n)}_{\text{only local exch.}} \tag{3.82}$$

we can see that all DFT exchange is first replaced by the improved GW exchange. The due to the GW Doublecounting the local exchange of the correlated subspace is subtracted, and then again the local impurity exchange is added.

There is still some local exchange in the term $\Sigma^{XC}_{GW}(k, i\omega_n) - \Sigma^{DC}_{GW}(i\omega_n)$ but it is originating from outside the correlated subspace or from couplings between the subspace and the remaining space, which is not contained in $\Sigma_{imp}(i\omega_n)$.

The GW doublecounting approaches the local Fock part in the large $i\omega_n$ limit, which means that we simply get the unscreened Fock-exchange values (compare with Section 3.2)

$$\lim_{i\omega_n \to \infty} \Sigma^{DC}_{GW,L}(i\omega_n) = -\frac{1}{\beta} \sum_{i\nu_n} \sum_{L'} G_{loc,L'}(i\omega_n - i\nu_n) V_{loc,LL'LL'} \tag{3.83}$$

$$= -\sum_{L'} n_L V_{loc,LL'LL'}. \tag{3.84}$$

When performing a pure DMFT calculation where no GW Selfenergy is added, we do not subtract the exchange correlation potential $V_{XC}$. Then we should subtract the full local Hartree **and** Fock exchange terms. By this, the local Hartree and Fock exchange terms are replaced by the DMFT impurity result and there is at least no doublecounting with respect to these terms.

# 4 Hartree- and Exchange term

In the GW+DMFT cycle we add the GW and the DMFT Selfenergy to the DFT Green's function to build up the final interacting Green's function

$$G(k,i\omega_n) = \big[\mathbb{1}(i\omega_n+\mu) - H^{DFT}(k) + v^{XC}(k) + \Sigma^{Hartree}_{DFT} - \Sigma^{XC}_{GW}(k,i\omega_n) + \Sigma^{XC}_{GW,imp}(i\omega_n) - \Sigma_{imp}(i\omega_n)\big]^{-1}, \tag{4.1}$$

where $\Sigma^{Hartree}_{DFT}$ is the Hartree term calculated in DFT. The GW Selfenergy does not contain a Hartree component, but the DMFT Selfenergy $\Sigma_{imp}(i\omega_n)$ does, which leads to a doublecounting of the Hartree term. Therefore, the DFT Hartree part is subtracted via $\Sigma^{Hartree}_{DFT}$.

In general we can expect charge transfer when applying the DMFT Method to the correlated orbitals, so the Hartree term is also expected to change. Therefore, we will replace the Hartree term completely by the one from DMFT.

We now derive the expression for the Hartree and exchange terms contained in DFT in a local orbital basis. The derivation follows the ideas of Haule PRL 115, 196403 (2015). We assume a constant interaction for the derivation, and then show what has to be modified when the interactions become frequency dependent in section 5.

## 4.1 Hartree term

The Hartree energy has the general form

$$E^H[\rho] = \frac{1}{2}\int \mathrm{d}\mathbf{r}\mathrm{d}\mathbf{r}'\,\rho(\mathbf{r})V_C(\mathbf{r}-\mathbf{r}')\rho(\mathbf{r}') \tag{4.2}$$

$$= \frac{1}{2}\int \mathrm{d}\mathbf{r}\mathrm{d}\mathbf{r}'\,\frac{\rho(\mathbf{r})\rho(\mathbf{r}')}{|\mathbf{r}-\mathbf{r}'|}, \tag{4.3}$$

where $\rho(\mathbf{r})$ is the sum of all spin-components

$$\rho(\mathbf{r}) = \rho_\uparrow(\mathbf{r}) + \rho_\downarrow(\mathbf{r}). \tag{4.4}$$

In order to evaluate these term for DMFT we introduce a local orbital basis $|\chi^\sigma_m\rangle$, and replace the bare Coulomb interaction $V_C(\mathbf{r}-\mathbf{r}')$ by an effective screened Coulomb interaction $V_{DMFT}(\mathbf{r}-\mathbf{r}')$. This leads to

$$E^H[\rho] = \frac{1}{2}\int \mathrm{d}\mathbf{r}\mathrm{d}\mathbf{r}'\,\rho(\mathbf{r})V_C(\mathbf{r}-\mathbf{r}')\rho(\mathbf{r}') \tag{4.5}$$

$$= \frac{1}{2}\sum_{\substack{klmn\\ \sigma\sigma'}}\int \mathrm{d}\mathbf{r}\mathrm{d}\mathbf{r}'\,\langle\mathbf{r}|\chi^\sigma_k\rangle\langle\chi^\sigma_k|\rho|\chi^\sigma_l\rangle\langle\chi^\sigma_l|\mathbf{r}\rangle V_{DMFT}(\mathbf{r}-\mathbf{r}') \times \langle\mathbf{r}'|\chi^{\sigma'}_m\rangle\langle\chi^{\sigma'}_m|\rho|\chi^{\sigma'}_n\rangle\langle\chi^{\sigma'}_n|\mathbf{r}'\rangle \tag{4.6}$$

$$= \frac{1}{2}\sum_{\substack{klmn\\ \sigma\sigma'}}\int \mathrm{d}\mathbf{r}\mathrm{d}\mathbf{r}'(\chi^\sigma_l)^*(\mathbf{r})(\chi^{\sigma'}_n)^*(\mathbf{r}')V_{DMFT}(\mathbf{r}-\mathbf{r}')\chi^{\sigma'}_m(\mathbf{r}')\chi^\sigma_k(\mathbf{r}) \times \langle\chi^\sigma_k|\rho|\chi^\sigma_l\rangle\langle\chi^{\sigma'}_m|\rho|\chi^{\sigma'}_n\rangle. \tag{4.7}$$

In the last equation we can now identify the matrix elements of the local screened Coulomb interaction

$$\langle ln|U|km\rangle = \int \mathrm{d}\mathbf{r}\mathrm{d}\mathbf{r}'(\chi_l^\sigma)^*(\mathbf{r})(\chi_n^{\sigma'})^*(\mathbf{r}')V_{DMFT}(\mathbf{r}-\mathbf{r}')\chi_m^{\sigma'}(\mathbf{r}')\chi_k^\sigma(\mathbf{r}), \tag{4.8}$$

and the DMFT density matrix

$$\langle \chi_k^\sigma|\rho|\chi_l^\sigma\rangle = n_{kl}^\sigma. \tag{4.9}$$

With this, the Hartree energy takes on the form

$$E^{DMFT} = \frac{1}{2}\sum_{\substack{klmn\\ \sigma\sigma'}} \langle ln|U|km\rangle\, n_{kl}^\sigma n_{mn}^{\sigma'}. \tag{4.10}$$

In the impurity model we restrict ourselves to diagonal density matrices, which leads to

$$E_{DMFT}^H = \frac{1}{2}\sum_{\substack{km\\ \sigma\sigma'}} \langle km|U|km\rangle\, n_k^\sigma n_m^{\sigma'}. \tag{4.11}$$

This leads to the following Hartree part of the Selfenergy in DMFT

$$\begin{aligned}
\Sigma_{l\sigma}^{H,DMFT} &= \frac{\partial}{\partial n_l^\sigma} E_{DMFT}^H && (4.12)\\
&= \frac{1}{2}\sum_{m,\sigma'} \langle lm|U|lm\rangle\, n_m^{\sigma'} + \frac{1}{2}\sum_{k,\sigma'} \langle kl|U|kl\rangle\, n_k^{\sigma'} && (4.13)\\
&= \sum_{m,\sigma'} \langle lm|U|lm\rangle\, n_m^{\sigma'} && (4.14)\\
&= U_0(n_l^\uparrow + n_l^\downarrow) + \sum_{m\neq l}(U_0 - 2J_{lm})(n_m^\uparrow + n_m^\downarrow). && (4.15)
\end{aligned}$$

## 4.2 Exchange term

The exact exchange energy has the general form

$$\begin{aligned}
E^X[\rho] &= -\frac{1}{2}\sum_\sigma \int \mathrm{d}\mathbf{r}\mathrm{d}\mathbf{r}'\, \rho_\sigma(\mathbf{r},\mathbf{r}')V_C(\mathbf{r}-\mathbf{r}')\rho_\sigma(\mathbf{r}',\mathbf{r}) && (4.16)\\
&= -\frac{1}{2}\sum_\sigma \int \mathrm{d}\mathbf{r}\mathrm{d}\mathbf{r}'\, \frac{\rho_\sigma(\mathbf{r},\mathbf{r}')\rho_\sigma(\mathbf{r}',\mathbf{r})}{|\mathbf{r}-\mathbf{r}'|}. && (4.17)
\end{aligned}$$

In order to evaluate these term for DMFT we introduce a local orbital basis $|\chi_m^\sigma\rangle$, and replace the bare Coulomb interaction $V_C(\mathbf{r}-\mathbf{r}')$ by an effective screened Coulomb

interaction $V_{DMFT}(\mathbf{r}-\mathbf{r}')$. This leads to

$$E^X[\rho] = -\frac{1}{2}\sum_\sigma \int \mathrm{d}\mathbf{r}\mathrm{d}\mathbf{r}'\, \rho_\sigma(\mathbf{r},\mathbf{r}')V_{DMFT}(\mathbf{r}-\mathbf{r}')\rho_\sigma(\mathbf{r}',\mathbf{r}) \tag{4.18}$$

$$= -\frac{1}{2}\sum_{\substack{klmn\\ \sigma}} \int \mathrm{d}\mathbf{r}\mathrm{d}\mathbf{r}'\, \langle\mathbf{r}|\chi_k^\sigma\rangle \langle\chi_k^\sigma|\rho_\sigma|\chi_l^\sigma\rangle \langle\chi_l^\sigma|\mathbf{r}'\rangle\, V_{DMFT}(\mathbf{r}-\mathbf{r}') \times \langle\mathbf{r}'|\chi_m^\sigma\rangle \langle\chi_m^\sigma|\rho_\sigma|\chi_n^\sigma\rangle \langle\chi_n^\sigma|\mathbf{r}\rangle \tag{4.19}$$

$$= -\frac{1}{2}\sum_{\substack{klmn\\ \sigma}} \int \mathrm{d}\mathbf{r}\mathrm{d}\mathbf{r}'\, (\chi_n^\sigma)^*(\mathbf{r})(\chi_l^\sigma)^*(\mathbf{r}')V_{DMFT}(\mathbf{r}-\mathbf{r}')\chi_m^\sigma(\mathbf{r}')\chi_k^\sigma(\mathbf{r}) \times \langle\chi_m^\sigma|\rho_\sigma|\chi_n^\sigma\rangle \langle\chi_k^\sigma|\rho_\sigma|\chi_l^\sigma\rangle\,. \tag{4.20}$$

In the last equation we can now identify the matrix elements of the local screened Coulomb interaction

$$\langle nl|U|km\rangle = \int \mathrm{d}\mathbf{r}\mathrm{d}\mathbf{r}'\, (\chi_n^\sigma)^*(\mathbf{r})(\chi_l^\sigma)^*(\mathbf{r}')V_{DMFT}(\mathbf{r}-\mathbf{r}')\chi_m^\sigma(\mathbf{r}')\chi_k^\sigma(\mathbf{r}), \tag{4.21}$$

and the DMFT density matrix

$$\langle\chi_m^\sigma|\rho_\sigma|\chi_n^\sigma\rangle = n_{mn}^\sigma. \tag{4.22}$$

With this, the exchange energy takes on the form

$$E_{DMFT}^X = -\frac{1}{2}\sum_{\substack{klmn\\ \sigma}} \langle nl|U|km\rangle\, n_{mn}^\sigma n_{kl}^\sigma. \tag{4.23}$$

In the impurity model we restrict ourselves to diagonal density matrices, which leads to

$$E_{DMFT}^X = -\frac{1}{2}\sum_{mk,\sigma} \langle mk|U|km\rangle\, n_m^\sigma n_k^\sigma. \tag{4.24}$$

This leads to the following exchange part of the Selfenergy in DMFT

$$\Sigma_{l\sigma}^{X,DMFT} = \frac{\partial}{\partial n_l^\sigma} E_{DMFT}^X \tag{4.25}$$

$$= -\frac{1}{2}\sum_k \langle lk|U|kl\rangle\, n_k^\sigma - \frac{1}{2}\sum_m \langle ml|U|lm\rangle\, n_m^\sigma \tag{4.26}$$

$$= -\sum_k \langle lk|U|kl\rangle\, n_k^\sigma \tag{4.27}$$

$$= -U_0\, n_l^\sigma - \sum_{k\neq l} J_{lk}\, n_k^\sigma. \tag{4.28}$$

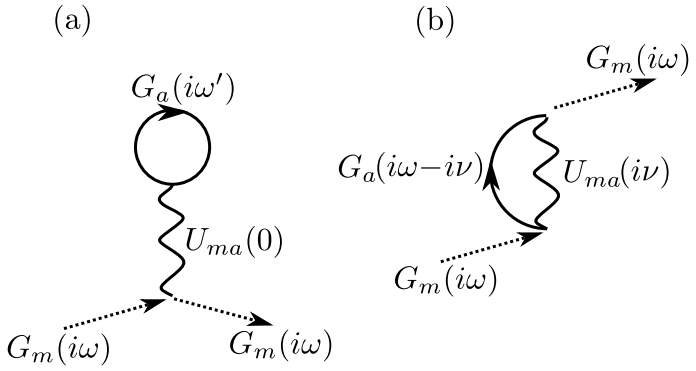


Figure 2: The local Hartree (a) and Fock diagram (b)

### 4.3 Hartree + exchange Selfenergy

For consistency checks, we add up the Hartree and the exchange contribution to the Selfenergy and obtain

$$\Sigma_{l\sigma}^{H,DMFT} + \Sigma_{l\sigma}^{X,DMFT} = U_0 n_l^{\bar{\sigma}} + \sum_{m \neq l} (U_0 - 2J_{lm}) n_m^{\bar{\sigma}} + \sum_{m \neq l} (U_0 - 3J_{lm}) n_m^{\sigma} \tag{4.29}$$

$$= \lim_{\omega_n \to \infty} \Sigma^{DMFT}(i\omega_n), \tag{4.30}$$

which is identical to the high-frequency limit of the true DMFT Selfenergy. This term is also equal to the sum of all first order diagrams to the DMFT Selfenergy, i.e. the Hartree- and the Fock diagram.

## 5 Hartree+Fock term in DMFT with Dynamical interactions

In the case of dynamical interactions $U(i\omega_n)$ in the screened Coulomb matrix elements recover their bare values for large frequencies. This leads to a slightly different expression for the Hartree and Fock term of the Selfenergy when solving the impurity model.

In our case, when we only use a frequency dependent monopole term $F_0$, all elements of the Coulomb interaction matrix have the same frequency dependence and only differ in a constant spin- and orbital dependent offset. This frequency dependence is described by $K(\tau)$, as defined in section 8.1. $K'(\tau) = \partial_\tau K(\tau)$, has the following form at $\tau = 0^+$

$$K'(0^+) = \frac{1}{2} \left[ V_{bare} - U(0) \right] \tag{5.1}$$

$$= \frac{1}{2} \left[ U(\infty) - U(0) \right]. \tag{5.2}$$

Since only the monopole term $F_0$ is frequency dependent, this results in

$$K'(0^+) = \frac{1}{2}\left[F_0(\infty) - F_0(0)\right] \tag{5.3}$$

which is spin- and orbital independent.

## 5.1 Hartree Term

We start by evaluating the Hartree diagram, shown in Fig. 2 (a).

$$\begin{aligned}
\Sigma^H_{m\sigma}(i\omega) &= \frac{1}{\beta}\sum_{a\sigma'}\sum_{i\omega'_n} U_{ma}(0) G_{a\sigma'}(i\omega'_n) && (5.4)\\
&= \sum_{a\sigma'} U_{ma}(0) n_{a\sigma'} && (5.5)\\
&= \sum_{a\sigma'} \left[U_{ma}(0) - U_{ma}(\infty) + U_{ma}(\infty)\right] n_{a\sigma'} && (5.6)\\
&= \sum_{a\sigma'} \left[U_{ma}(0) - U_{ma}(\infty)\right] n_{a\sigma'} + \sum_{a\sigma'} U_{ma}(\infty) n_{a\sigma'} && (5.7)\\
&= -2K'(0^+)N + \sum_{a\sigma'} U_{ma}(\infty) n_{a\sigma'}, && (5.8)
\end{aligned}$$

where $N = \sum_{a\sigma} n_{a\sigma}$.

## 5.2 Fock Term

We start by evaluating the Fock diagram, shown in Fig. 2 (b).

$$\begin{aligned}
\Sigma^F_{m\sigma}(i\omega) &= -\frac{1}{\beta}\sum_{a}\sum_{i\nu_n} J_{ma}(i\nu_n) G_{a\sigma}(i\omega_n - i\nu_n) && (5.9)\\
&= -\frac{1}{\beta}\sum_{a}\sum_{i\nu_n} \left[J_{ma}(i\nu_n) - J_{ma}(\infty) + J_{ma}(\infty)\right] G_{a\sigma}(i\omega_n - i\nu_n) && (5.10)\\
&= -\frac{1}{\beta}\sum_{a}\sum_{i\nu_n} J_{ma}(\infty) G_{a\sigma}(i\omega_n - i\nu_n)\\
&\quad - \frac{1}{\beta}\sum_{a} \underbrace{\sum_{i\nu_n} \left[J_{ma}(i\nu_n) - J_{ma}(\infty)\right] G_{a\sigma}(i\omega_n - i\nu_n)}_{\to 0 \text{ for } i\omega\to\infty} && (5.11)\\
&= -\sum_{a} J_{ma}(\infty) n_{a\sigma}. && (5.12)
\end{aligned}$$

## 5.3 Hartree+Fock Term

This leads to the final expression

$$\Sigma^H_{m\sigma} = -2K'(0^+)N + \sum_{a\sigma'} U_{ma}(\infty) n_{a\sigma'} \tag{5.13}$$

$$\Sigma^F_{m\sigma} = -\sum_{a} J_{ma}(\infty) n_{a\sigma} \tag{5.14}$$

$$\Sigma^{HF}_{m\sigma} = -2K'(0^+)N + \sum_{a} U_{ma}(\infty) n_{a\bar{\sigma}} + \sum_{a} [U_{ma}(\infty) - J_{ma}(\infty)] n_{a\sigma}. \tag{5.15}$$

# 6 Product basis

In the GW formalism we encounter objects such as the inverse dielectric function

$$\epsilon^{-1}, \tag{6.1}$$

which is a two-particle operator. The standard way to specify the action of a two-particle operator is to start from a complete orthonormal single-particle basis $\{|i\rangle\}$, where

$$\langle \mathbf{r}|i\rangle = \psi_i(\mathbf{r}), \tag{6.2}$$

with a complex valued function $\psi_i : R^3 \to \mathbb{C}$. Then one introduces a two-particle basis $\{|ij\rangle\}$, which is composed of the single-particle states via

$$\langle \mathbf{r}\mathbf{r}'|ij\rangle = \Big( \langle \mathbf{r}| \otimes \langle \mathbf{r}'| \Big) \Big( |i\rangle \otimes |j\rangle \Big) \tag{6.3}$$

$$= \psi_i(\mathbf{r})\psi_j(\mathbf{r}'). \tag{6.4}$$

In this basis, any two-particle operator $A$ can be represented as a rank-4 tensor by its action on the two-particle basis states

$$A_{ijkl} = \langle ij|A|kl\rangle \tag{6.5}$$

$$= \int\int \mathrm{d}\mathbf{r}\mathrm{d}\mathbf{r}'\, \psi^*_i(\mathbf{r})\psi^*_j(\mathbf{r}')A(\mathbf{r},\mathbf{r}')\psi_l(\mathbf{r}')\psi_k(\mathbf{r}), \tag{6.6}$$

where we have assumed that

$$\langle \mathbf{r}\mathbf{r}'|A|\mathbf{r}''\mathbf{r}'''\rangle = A(\mathbf{r},\mathbf{r}')\delta(\mathbf{r}-\mathbf{r}'')\delta(\mathbf{r}'-\mathbf{r}'''), \tag{6.7}$$

which applies to the Coulomb interaction operator and all other operators we will consider here.

Our goal is to obtain a matrix (rank-2) representation of the two-particle operator $A$, so that we can define a proper inverse $A^{-1}$ or a multiplication $AB$ between these operators. This is usually done in two ways:

## 6.1 Index combination

In the two-particle basis the structure of the Tensor-elements

$$A_{ijkl} = \langle ij|A|kl\rangle\,, \tag{6.8}$$

suggests that we could also interpret each basis state as

$$|a\rangle := |ij\rangle = |i\rangle \otimes |j\rangle\,, \tag{6.9}$$

with a single basis state $|a\rangle$, where the index $a$ now runs over $N^2$ values if we have $N$ single particle states $|i\rangle$. In this notation, we can indeed write the tensor elements as matrix elements

$$\begin{aligned} A_{ab} &= \langle a|A|b\rangle && (6.10)\\ &= \langle ij|A|kl\rangle && (6.11)\\ &= A_{(ij)(kl)}. && (6.12) \end{aligned}$$

### 6.1.1 Properties and consistency

The combination of the two left, the "outgoing" indices $ij$ and the right, the "incoming" $kl$ is in principle arbitrary. We could also combine the indices $ik$ of the first partcile and $jl$ of the second particle. Though, the $(ij)(kl)$ combination should be preferrable, since it does not mix vectors $|i\rangle$ with their dual counterpart $\langle i|$.

Furthermore, in cases where we want to apply this scheme, the tensor operations can indeed be rewritten as a matrix multiplication in the combined "ingoing-outgoing" index notation. For example the screened interaction $W$ is given by

$$\begin{aligned} W_{ijkl} &= [v + vPW]_{ijkl} && (6.13)\\ &= v_{ijkl} + \sum_{mnop} v_{ijmn} P_{mnop} W_{opkl}, && (6.14) \end{aligned}$$

with the bare interaction $v$ and the polarization $P$. Using the combined index notation we get the representation

$$\begin{aligned} W_{ab} &= W_{(ij)(kl)} && (6.15)\\ &= v_{(ij)(kl)} + \sum_{(mn)(op)} v_{(ij)(mn)} P_{(mn)(op)} W_{(op)(kl)} && (6.16)\\ &= v_{ab} + \sum_{cd} v_{ac} P_{cd} W_{da} && (6.17)\\ &= [v + vPW]_{ab}, && (6.18) \end{aligned}$$

where $vPW$ is to be understood as the matrix product of $v$, $P$ and $W$ in the combined index notation.

### 6.1.2 Tensor inverse

Now let us try to obtain a closed expression of $W$ satisfying this expression, which is not possible in the 4-index tensor notation. For this, we need to define first an object $\mathbb{1}$ that serves as the identity element, which then will allow us to poperly define an inverse of a matrix in the combined index notation. The identity element should have the following property

$$\mathbb{1}A = A = A\mathbb{1}, \tag{6.19}$$

where $A$ is a two-particle tensor, which means

$$\begin{aligned} A_{(ij)(kl)} &= A_{ab} && (6.20)\\ &= [\mathbb{1}A]_{ab} && (6.21)\\ &= \sum_c \mathbb{1}_{ac} A_{ca} && (6.22)\\ &= \sum_{mn} \mathbb{1}_{(ij)(mn)} A_{(mn)(kl)}. && (6.23) \end{aligned}$$

From this we conclude that

$$\begin{aligned} \mathbb{1}_{(ij)(mn)} &= \delta_{im}\delta_{jn} && (6.24)\\ \Rightarrow \mathbb{1}_{ac} &= \delta_{ac}, && (6.25) \end{aligned}$$

which leads to the natural definition of the identity element in the combined index notation. It can be directly seen that also $A\mathbb{1} = A$ is fulfilled.

From this we can define the inverse $A^{-1}$ as the standard matrix inverse in the combined index notation that fulfills

$$A^{-1}A = AA^{-1} = \mathbb{1}, \tag{6.26}$$

since

$$\begin{aligned} [A^{-1}A]_{(ij)(kl)} &= [A^{-1}A]_{ab} && (6.27)\\ &= \delta_{ab} && (6.28)\\ &= \delta_{ik}\delta_{kl} && (6.29)\\ &= \mathbb{1}_{(ij)(kl)} && (6.30) \end{aligned}$$

With this, we can finally solve the equation above for the screened interaction

$$\begin{aligned} W &= v + vPW && (6.31)\\ \Rightarrow (\mathbb{1} - vP)W &= v && (6.32)\\ \Rightarrow W &= (\mathbb{1} - vP)^{-1}v, && (6.33) \end{aligned}$$

By contruction, the tensor elements $W_{ijkl} = [(\mathbb{1} - vP)^{-1}v]_{ijkl}$ will now satisfy the equation above for the screened interaction.

### 6.1.3 Problems

Possible problems are:

- A two-particle operator diagonal in position representation cannot be inverted in the combined index-notation! This can be for example a purely local Coulomb interaction!

  Consider

  $$\langle \mathbf{r}\mathbf{r}'|A|\mathbf{r}''\mathbf{r}'''\rangle = A(\mathbf{r})\delta(\mathbf{r}-\mathbf{r}')\delta(\mathbf{r}-\mathbf{r}'')\delta(\mathbf{r}'-\mathbf{r}'''), \tag{6.34}$$

  and we assume that $A(\mathbf{r}) = a > 0$ constant, *i.e.* it does not matter where the particles interact. As long as their positions are identical they pick up a factor $a$.

  This leads to the following tensor elements

  $$\begin{aligned} A_{ijkl} &= \langle ij|A|kl\rangle && (6.35)\\ &= \int\int \mathrm{d}\mathbf{r}\mathrm{d}\mathbf{r}'\, \psi_i^*(\mathbf{r})\psi_j^*(\mathbf{r}')a\delta(\mathbf{r}-\mathbf{r}')\psi_l(\mathbf{r}')\psi_k(\mathbf{r}) && (6.36)\\ &= a\int \mathrm{d}\mathbf{r}\, \psi_i^*(\mathbf{r})\psi_j^*(\mathbf{r})\psi_l(\mathbf{r})\psi_k(\mathbf{r}). && (6.37) \end{aligned}$$

  For the case of real wave functions we see that we always get a non-zero contribution when we pair two indices with one another, leading to an integral of the form

  $$a\int \mathrm{d}\mathbf{r}\, \psi_m^2(\mathbf{r})\psi_n^2(\mathbf{r}) \neq 0 \tag{6.38}$$

  For the example of $N = 2$ single-particle states $\psi_i(\mathbf{r})$, we can choose two out of four indices to pair, then the last one has to be paired with $N = 2$ choices for the index, leading to 8 combinations which are at least non-zero. In the combined index notation we then can arrive at the following matrix (Note: I have confirmed this numerically for a few basis sets)

  $$A = a\begin{pmatrix} c_1 & 0 & 0 & c_3 \\ 0 & c_2 & c_2 & 0 \\ 0 & c_2 & c_2 & 0 \\ c_3 & 0 & 0 & c_4 \end{pmatrix}, \tag{6.39}$$

  where we can immediately see that this matrix cannot be inverted since two columns are linearly dependent (even identical).

- A "constant" operator $A(\mathbf{r},\mathbf{r}') = c \neq 0$ can be inverted! (See discussion in next section)

## 6.2 Aryasetiawan-style

### 6.2.1 Defining the new basis set

We start by rewriting the equation for the tensor elements in the two-particle basis in the following way

$$\langle ij|A|kl\rangle = \int\int \mathrm{d}\mathbf{r}\mathrm{d}\mathbf{r}'\, \psi_i^*(\mathbf{r})\psi_j^*(\mathbf{r}')A(\mathbf{r},\mathbf{r}')\psi_l(\mathbf{r}')\psi_k(\mathbf{r}) \tag{6.40}$$

$$= \int\int \mathrm{d}\mathbf{r}\mathrm{d}\mathbf{r}'\, \psi_i^*(\mathbf{r})\psi_k(\mathbf{r})A(\mathbf{r},\mathbf{r}')\psi_j^*(\mathbf{r}')\psi_l(\mathbf{r}') \tag{6.41}$$

$$= \int\int \mathrm{d}\mathbf{r}\mathrm{d}\mathbf{r}'\, \underbrace{\Big(\psi_k^*(\mathbf{r})\psi_i(\mathbf{r})\Big)^*}_{B_a^*(\mathbf{r})} A(\mathbf{r},\mathbf{r}') \underbrace{\psi_j^*(\mathbf{r}')\psi_l(\mathbf{r}')}_{B_b(\mathbf{r}')} \tag{6.42}$$

$$= \langle B_a|A|B_b\rangle\,. \tag{6.43}$$

From these observation we see that we should define new basis states $\{B_a\}$ by the product of the single-particle states by

$$\langle \mathbf{r}|B_a\rangle := \psi_i^*(\mathbf{r})\psi_j(\mathbf{r}), \tag{6.44}$$

where the index $a := a(i,j)$ lables the combination of the indices $i,j$. As a result, for a finite number of single-particle states $N = \dim\{|i\rangle\}$, we have $N^2$ new basis states $\{B_a\}$, and could define the relation between the indices as

$$a(i,j) := iN + j. \tag{6.45}$$

Though, the new set $\{B_a\}$ is *not* a basis, since it is overcomplete/linearly dependent and in addition not orthonormal. For example if there exist at least two real single-particle basis functions $\psi_i, \psi_j$, one has

$$\psi_i(\mathbf{r})\psi_j(\mathbf{r}) = B_a(\mathbf{r}) = B_b(\mathbf{r}) = \psi_j(\mathbf{r})\psi_i(\mathbf{r}), \tag{6.46}$$

where $a \neq b$. Also, for a states with indices $a(i,i)$ and $b(i,i)$, which leads to

$$\langle B_a|B_b\rangle = \int \mathrm{d}\mathbf{r}\, \psi_i^*(\mathbf{r})\psi_i(\mathbf{r})\psi_j^*(\mathbf{r})\psi_j(\mathbf{r}) \tag{6.47}$$

$$= \int \mathrm{d}\mathbf{r}\, |\psi_i(\mathbf{r})|^2|\psi_j(\mathbf{r})|^2 \tag{6.48}$$

which is usually larger than zero for $a \neq b$, i.e. $i = j$ and not equal to 1 in case $a = b$, i.e. $i \neq j$.

The overlap matrix for the new set $\{B_a\}$ is therefore different from the unit matrix. If we define

$$v := \begin{pmatrix} |B_1\rangle & |B_2\rangle & |B_3\rangle & \cdots & |B_{N^2}\rangle \end{pmatrix}, \tag{6.49}$$

then the overlap matrix can be written as

$$O = v^\dagger \cdot v, \tag{6.50}$$

since

$$O_{ab} = (v^\dagger \cdot v)_{ab} \tag{6.51}$$
$$= \langle B_a | B_b \rangle \,. \tag{6.52}$$

Due to the overcompleteness, some columns of $O$ will not be linear independent, i.e. some of the Eigenvalues $\lambda_i$ of $O$ will be equal to zero.

### 6.2.2 Reduction of the basis set and reorthonormalization

After diagonalizing $O$ to obtain the Eigenvectors $o_1, o_2, ..., o_{N^2}$, we throw away the ones with Eigenvalue zero and set up the matrices

$$U = \begin{pmatrix} o_1 & o_2 & o_3 & \cdots o_{N_r} \end{pmatrix} \in \mathbb{C}^{N^2 \times N_r}, \tag{6.53}$$

where $N_r \leq N^2$ is the number of Eigevectors with nonzero Eigenvalue, and

$$D^{-1/2} := \mathrm{diag}({\lambda_1}^{-1/2},\ {\lambda_2}^{-1/2},\ {\lambda_3}^{-1/2},\ \cdots,\ {\lambda_{N_r}}^{-1/2}) \in \mathbb{R}^{N_r \times N_r}, \tag{6.54}$$

where $\lambda_i$ are the nonzero Eigenvalues of $O$.

The elements of the following vector

$$\tilde{v} := vUD^{-1/2}, \tag{6.55}$$

will then yield a new set of $N_r$ basis functions which are complete and orthonormal, as can be seen from the new overlap matrix

$$\tilde{O} = \tilde{v}^\dagger \cdot \tilde{v} \tag{6.56}$$
$$= D^{-1/2} U^\dagger (v^\dagger \cdot v) U D^{-1/2} \tag{6.57}$$
$$= D^{-1/2} \underbrace{U^\dagger O U}_{=D} D^{-1/2} \tag{6.58}$$
$$= \mathbb{1} \in \mathbb{R}^{N_r \times N_r}. \tag{6.59}$$

*Remark:* To reduce the size of the basis for computational efficiency, one can also exclude Eigenvectors with a finite, but small Eigenvalue, i.e. below some treshhold $\delta > \lambda_i$. Then the new basis will only be approximately complete and orthonormal, but the error can be controlled by choosing $\delta$ sufficiently small.

### 6.2.3 Product basis matrix elements

After having obtained the new complete orthonormal basis $\{\tilde{B}_a\}$, the matrix elements of any two-particle operator are then given as

$$A_{ab} = \langle \tilde{B}_a | A | \tilde{B}_b \rangle \tag{6.60}$$
$$= \int\int \mathrm{d}\mathbf{r}\mathrm{d}\mathbf{r}'\, \tilde{B}_a^*(\mathbf{r}) A(\mathbf{r}, \mathbf{r}') \tilde{B}_b(\mathbf{r}'). \tag{6.61}$$

The representation of $A$ in the product basis is then given as

$$A = \sum_{a,b} |\tilde{B}_a\rangle\, A_{ab}\, \langle \tilde{B}_b| \,. \tag{6.62}$$

or in the position representation DOES THIS MAKE SENSE?

$$A(\mathbf{r},\mathbf{r}') = \sum_{a,b} \langle \mathbf{r}|\tilde{B}_a\rangle \, A_{ab} \, \langle \tilde{B}_b|\mathbf{r}'\rangle \tag{6.63}$$

$$= \sum_{a,b} \tilde{B}_a(\mathbf{r}) A_{ab} \tilde{B}^*_b(\mathbf{r}'). \tag{6.64}$$

CHECK HERE IF BOTH REPRESENTATIONS LEAD TO THE SAME RESULT!!! The product basis should recover the right A(r-r'), shouldn't it? (I think so...) Can we actually prove this?

### 6.2.4 Switching between the product and the two-particle basis

If we want to obtain the original tensor representation of a two-particle operator in the product basis, we have to evaluate DOES THIS MAKE SENSE?

$$A_{ijkl} = \langle ij|A|kl\rangle \tag{6.65}$$

$$= \int\int \mathrm{d}\mathbf{r}\mathrm{d}\mathbf{r}' \, \psi^*_i(\mathbf{r})\psi^*_j(\mathbf{r}')A(\mathbf{r},\mathbf{r}')\psi_l(\mathbf{r}')\psi_k(\mathbf{r}) \tag{6.66}$$

$$= \sum_{a,b} \int\int \mathrm{d}\mathbf{r}\mathrm{d}\mathbf{r}' \, \psi^*_i(\mathbf{r})\psi^*_j(\mathbf{r}')\tilde{B}_a(\mathbf{r})A_{ab}\tilde{B}^*_b(\mathbf{r}')\psi_l(\mathbf{r}')\psi_k(\mathbf{r}). \tag{6.67}$$

The other way round, if we have a two-particle operator given in the two-particle basis, the product basis representation can be obtained by

$$A_{ab} = \langle \tilde{B}_a|A|\tilde{B}_b\rangle \tag{6.68}$$

$$= \int\int \mathrm{d}\mathbf{r}\mathrm{d}\mathbf{r}' \, \tilde{B}^*_a(\mathbf{r})A(\mathbf{r},\mathbf{r}')\tilde{B}_b(\mathbf{r}') \tag{6.69}$$

$$= \sum_{ijkl} \int\int \mathrm{d}\mathbf{r}\mathrm{d}\mathbf{r}' \, \tilde{B}^*_a(\mathbf{r})\psi_i(\mathbf{r})\psi_j(\mathbf{r}')A_{ijkl}\psi^*_l(\mathbf{r}')\psi^*_k(\mathbf{r})\tilde{B}_b(\mathbf{r}'). \tag{6.70}$$

### 6.2.5 Tensor inverse

Since in the product basis any two-particle operator can now be represented as a matrix/rank-2 tensor, we can finally define its inverse $\tilde{A}^{-1}$ as the standard Matrix inverse, which then in the product basis fulfils the property

$$(\tilde{A}^{-1}A)_{ab} = \langle \tilde{B}_a|\tilde{A}^{-1}A|\tilde{B}_b\rangle \tag{6.71}$$

$$= \delta_{ab}. \tag{6.72}$$

In the position representation

$$\langle \mathbf{r}|\tilde{A}^{-1}A|\mathbf{r}'\rangle = \sum_{a,b} \langle \mathbf{r}|\tilde{B}_a\rangle \, (\tilde{A}^{-1}A)_{ab} \, \langle \tilde{B}_b|\mathbf{r}'\rangle \tag{6.73}$$

$$= \sum_{a,b} \langle \mathbf{r}|\tilde{B}_a\rangle \, \delta_{ab} \, \langle \tilde{B}_b|\mathbf{r}'\rangle \tag{6.74}$$

$$= \sum_{a} \langle \mathbf{r}|\tilde{B}_a\rangle \, \langle \tilde{B}_a|\mathbf{r}'\rangle \tag{6.75}$$

$$= \langle \mathbf{r}|\mathbf{r}'\rangle \tag{6.76}$$

$$= \delta(\mathbf{r}-\mathbf{r}'), \tag{6.77}$$

if the product basis is complete.

### 6.2.6 Problems

Possible problems are:

- A "constant" tensor of the form $A(\mathbf{r},\mathbf{r}') = c \neq 0$ cannot be inverted! I'm not sure, this is maybe correct behaviour?

  Let us assume we obtain a final basis state $|\tilde{B}_o\rangle$ in a one-dimensional system which is a real odd function in position representation, *i.e.*

  $$\tilde{B}_o(r) = -\tilde{B}_o(-r). \tag{6.78}$$

  For a constant tensor this leads to the following

  $$A_{ab} = c \int\int \mathrm{d}\mathbf{r}\mathrm{d}\mathbf{r}' \, \tilde{B}^*_a(\mathbf{r})\tilde{B}_b(\mathbf{r}') \tag{6.79}$$

  $$= c \left(\int \mathrm{d}\mathbf{r} \, \tilde{B}^*_a(\mathbf{r})\right)\left(\int \mathrm{d}\mathbf{r}' \, \tilde{B}_b(\mathbf{r}'),\right), \tag{6.80}$$

  *i.e.* the two integrations over the basis states decouple, and everytime $a$ or $b$ is equal to the real odd function $\tilde{B}_o$, we obtain zero. Therefore, the $o$-th column and row is equal to zero. Which means, we have at least one Eigenvalue equal to zero and, therefore, the tensor in the product basis cannot be inverted.

- The "identity" tensor of the form $\langle ij|A|kl\rangle = \delta_{ik}\delta_{jl}$ cannot be inverted! This can be seen from

  $$A_{ab} = \langle \tilde{B}_a|A|\tilde{B}_b\rangle \tag{6.81}$$

  $$= \sum_{ijkl} \int\int \mathrm{d}\mathbf{r}\mathrm{d}\mathbf{r}' \, \tilde{B}^*_a(\mathbf{r})\psi_i(\mathbf{r})\psi_j(\mathbf{r}')A_{ijkl}\psi^*_l(\mathbf{r}')\psi^*_k(\mathbf{r})\tilde{B}_b(\mathbf{r}') \tag{6.82}$$

  $$= \sum_{ij} \int\int \mathrm{d}\mathbf{r}\mathrm{d}\mathbf{r}' \, \tilde{B}^*_a(\mathbf{r})\psi_i(\mathbf{r})\psi_j(\mathbf{r}')\psi^*_j(\mathbf{r}')\psi^*_i(\mathbf{r})\tilde{B}_b(\mathbf{r}') \tag{6.83}$$

  $$= \sum_{ij} \left(\int \mathrm{d}\mathbf{r} \, \tilde{B}^*_a(\mathbf{r})|\psi_i(\mathbf{r})|^2\right)\left(\int \mathrm{d}\mathbf{r}' \, \tilde{B}_b(\mathbf{r}')|\psi_j(\mathbf{r}')|^2\right). \tag{6.84}$$

  If one basis function $\tilde{B}_a(\mathbf{r})$ is an odd function, the full column $a$ and row $a$ will be zero, so we have at least one Eigenvalue equal to zero and, therefore, the tensor in the product basis cannot be inverted.

# 7 The GW part

On the basis of $H^{DFT}$ a $G_0W_0$ calculation has to be performed on the full system. By this, the Selfenergy in the Kohn-Sham basis is obtained for all states

$$\Sigma_{\nu\nu'}(k,\omega) = [G_0W_0]_{\nu\nu'}(k,\omega). \tag{7.1}$$

By this, the GW estimate for the full interacting Green's function is given by

$$G^{GW}_{\nu\nu'}(k,\omega) = \left[\mathbb{1}(\omega+\mu+i\delta) - H^{DFT}(k) + v^{XC}(k) - \Sigma^{GW}(k,\omega)\right]^{-1}_{\nu\nu'}. \tag{7.2}$$

## 7.1 Output for DMFT

At this point the basis transformation to the local Wannier basis will be performed on the GW side. For the next step of the DMFT calculation one needs on a mesh in k-space in the full Brillouin zone:

- $\beta$: The inverse temperature used for defining $\omega_n = (2n+1)\pi/\beta$.
- $\epsilon_m(k)$: The eigenvalues of $H^{DFT}(k)$ in the Wannier basis for all relevant orbitals
- $\mu$: The chemical potential that yields the correct physical number of electrons $N_e$. It is not needed if all $\epsilon_m(k)$ are given with respect to the Fermi level. for $H^{DFT}$
- $v^{XC}_{mm'}(k)$: The value of the exchange-correlation potential in the Wannier basis for all relevant orbitals
- $\Sigma^{GW,XC}_{mm'}(k,i\omega)$: The exchange-correlation Selfenergy within GW in the Wannier basis for all relevant orbitals on imaginary frequencies $\omega$.
- $\Sigma^{GW,imp,XC}_{mm'}(i\omega) = -[G^{0,loc,L}W^{0,loc,L}]^{XC}_{mm'}$ The exchange-correlation selfenergy of the impurity model solved in GW, *i.e.* all indices and internal transitions restricted to the correlated subspace
- $V_{abcd}(q)$: The bare Coulomb interaction elements in the Wannier basis for all relevant orbitals. ?Do we have V in the product basis of the 3d orbitals? When do we construct this? IMPORTANT: IS the spin also incorporated or kept separate?
- $P^{GW}_{abcd}(q,i\nu)$: The polarization in the Wannier basis for all relevant orbitals on imaginary frequencies.?Do we have P in the product basis of the 3d orbitals? When do we construct this?
- $P^{GW,imp}_{abcd}(i\nu) = [G^{0,loc,L}G^{0,loc,L}]_{abcd}$ The polarization of the impurity model solved in GW, *i.e.* all indices and internal transitions restricted to the correlated subspace

*All output from the GW calculation will be in atomic units and has to be converted to eV!!*

# 8 The DMFT part

Within DMFT we then calculate a local correction $\Sigma^{DMFT}$ for a subset of correlated Wannier orbitals.

The input of the calculation will be the output of the GW calculation. First, one will usually apply a Wannier-interpolation of the GW data to obtain a fine k-mesh since the GW output will be given on a very coarse grid.

## 8.1 The self-consistency cycle

We then proceed as follows:

1. Make a first guess for the local DMFT impurity Selfenergy $\Sigma^{imp}$ and polarization $P^{imp}$, for example one can use the GW result

$$\Sigma^{imp}(i\omega_n) = \Sigma^{DC}_{GW}(i\omega_n) + \Sigma^{Hartree}_{DFT} \tag{8.1}$$
$$P^{imp}(i\nu_n) = P^{DC}_{GW}(i\nu_n). \tag{8.2}$$

   Please note that $\Sigma$ is a matrix in the orbital basis $\Sigma_{mm'}$ and $P$ is a tensor $P_{\alpha\beta}$ in the product basis $\{B_\alpha\}$, where $P, V$ and all further tensors are treated as standard matrices $P_{\alpha\beta} = \langle B_\alpha | P | B_\beta \rangle$, etc.

2. Set up the interacting Green's function $G$ and the screened interaction $W$, where the impurity component of the GW contribution for the correlated orbitals is replaced by the DMFT contribution.

$$G(k, i\omega_n) = \big[\mathbb{1}(i\omega_n + \mu) - H^{DFT}(k) + v^{XC}(k) + \Sigma^{Hartree}_{DFT} \tag{8.3}$$
$$- \Sigma^{XC}_{GW}(k, i\omega_n) + \Sigma^{DC}_{GW}(i\omega_n) - \Sigma_{imp}(i\omega_n)\big]^{-1} \tag{8.4}$$
$$W(q, i\nu_n) = \big[V^{-1}(q) - P_{GW}(q, i\nu_n) + P^{DC}_{GW}(i\nu_n) - P_{imp}(i\nu_n)\big]^{-1} \tag{8.5}$$

   Adjust the chemical potential $\mu$ in a way such that the desired filling

$$N_e = \lim_{\tau \to 0^-} \frac{1}{\beta N_k} \sum_{i\omega_n} \sum_{k,m} G_{mm}(k, i\omega_n) \mathrm{e}^{-i\omega_n \tau}. \tag{8.6}$$

   is obtained.

3. Calculate the local Green's function and the local screened interaction (for all orbitals)

$$G^{loc}(i\omega_n) = \frac{1}{N_k} \sum_k G(k, i\omega_n) \tag{8.7}$$
$$W^{loc}(i\nu_n) = \frac{1}{N_q} \sum_q W(q, i\nu_n). \tag{8.8}$$

   and then derive the Weiss field $\mathscr{G}$ and the effective interaction

$$\mathscr{G}(i\omega_n) = \big[[G^{loc}]^{-1}(i\omega_n) + \Sigma^{imp}(i\omega_n)\big]^{-1} \tag{8.9}$$
$$\mathcal{U}(i\nu_n) = \big[[W^{loc}]^{-1}(i\nu_n) + P^{imp}(i\nu_n)\big]^{-1}. \tag{8.10}$$

The Weiss field matrix $\mathscr{G}$ is not explicitly needed, so it is not necessary to invert the equation for $\mathscr{G}$ .

4. Calculate the Hybridization function

$$\Delta(i\omega_n) = i\omega_n + \tilde{\mu} - \mathscr{G}^{-1}(i\omega_n), \tag{8.11}$$

where the local chemical potential $\tilde{\mu}$ (which is orbital dependent!) is given by

$$\tilde{\mu} = \lim_{\omega_n \to \infty} \mathrm{Re}\left[\mathscr{G}^{-1}(i\omega_n)\right] \tag{8.12}$$

and transform $\Delta(i\omega_n)$ to the imaginary time axis $\tau$ by a Fourier transform

$$\Delta(\tau) = \frac{1}{\beta} \sum_{i\omega_n} \Delta(i\omega_n) \mathrm{e}^{-i\omega_n \tau}. \tag{8.13}$$

5. Transform the $\mathcal{U}_{\alpha\beta}(i\nu_n)$ matrix from the product basis to a two-particle tensor $\mathcal{U}_{ijkl}(i\nu_n)$ via

$$\mathcal{U}_{ijkl}(i\nu_n) = \sum_{\alpha\beta} \langle ij|B_\alpha\rangle \, \mathcal{U}_{\alpha\beta}(i\nu_n) \, \langle B_\beta|kl\rangle \tag{8.14}$$

$$= \sum_{\alpha\beta} O^{\alpha}_{ij} \mathcal{U}_{\alpha\beta}(i\nu_n) O^{\beta,*}_{kl}. \tag{8.15}$$

For now, we restrict ourselves to density-density interactions and use the parametrization in terms of Slater integrals.

Therefore, we extract

$$U_{avg}(i\nu_n) = \frac{1}{(2l+1)^2} \sum_{mm'} \mathcal{U}_{mm'mm'}(i\nu_n) = F_0(i\nu_n) \tag{8.16}$$

$$J_{avg}(i\nu_n) = U_{avg}(i\nu_n) - \frac{1}{2l(2l+1)} \sum_{mm'} \left(\mathcal{U}_{mm'mm'}(i\nu_n) - \mathcal{U}_{mm'm'm}(i\nu_n)\right) \tag{8.17}$$

$$= \frac{F_2(i\nu_n) + F_4(i\nu_n)}{14}, \tag{8.18}$$

Since the Hund's coupling does not depend strongly on frequency, we only tread the monopole term $F_0(i\nu_n) = U_{avg}(i\nu_n)$ as frequency dependent. Generate the $K(\tau), K'(\tau)$ functions from the retarded interaction via (see Chapter 8.3 for important high-frequency correction!)

$$K(\tau) = -\frac{2}{\beta} \sum_{n>0} \frac{F_0(i\nu_n) - F_0(0)}{\nu_n^2} (\cos(\nu_n \tau) - 1) \tag{8.19}$$

$$K'(\tau) = \frac{2}{\beta} \sum_{n>0} \frac{F_0(i\nu_n) - F_0(0)}{\nu_n} \sin(\nu_n \tau), \tag{8.20}$$

The static part of the interaction matrix is then generated from $U_{avg}(\infty)$ and $J_{avg}(0)$ by using the construction in terms of Slater integrals.

6. Use $\Delta_{mm'}(\tau), \tilde{\mu}_m, K(\tau), K'(\tau)$ and the density-density interaction matrix $U_{mm'}$ to solve the impurity model. We assume a diagonal hybridization in our case.

7. Obtain the new local Selfenergy $\Sigma^{imp}_{mm'}(i\omega_n)$ and the susceptibility $\chi^{imp}_{ijkl}(i\nu_n)$ from the impurity model. Transform the susceptibility from the two-particle basis to the product basis via

$$\chi^{imp}_{\alpha\beta}(i\nu_n) = \sum_{ijkl} \langle B_\alpha|ij\rangle \, \chi^{imp}_{ijkl}(i\nu_n) \, \langle kl|B_\beta\rangle \tag{8.21}$$

$$= \sum_{ijkl} O^{\alpha,*}_{ij} \chi^{imp}_{ijkl}(i\nu_n) O^{\beta}_{kl}, \tag{8.22}$$

and us the $\chi^{imp}_{\alpha\beta}(i\nu_n)$ matrix to calculate the updated impurity polarization and impurity screened interaction via

$$W^{imp}(i\nu_n) = \mathcal{U}(i\nu_n) - \mathcal{U}(i\nu_n)\chi^{imp}(i\nu_n)\mathcal{U}(i\nu_n) \tag{8.23}$$

$$P^{imp}(i\nu_n) = \mathcal{U}^{-1}(i\nu_n) - W^{imp,-1}(i\nu_n)$$

$$= -[\mathbb{1} - \chi^{imp}(i\nu_n)\mathcal{U}(i\nu_n)]^{-1}\chi^{imp}(i\nu_n). \tag{8.24}$$

or calculate first P,W and then transform to product basis? Then go back to step 2. Do we only need charge-charge susceptibility $\chi(\tau) = \langle n(\tau)n(0)\rangle$?? Phys.Reb.B.87,125149 says so?... Repeat until convergence is reached, i.e.

$$G^{imp}(i\omega_n) \stackrel{!}{=} G^{loc}(i\omega_n) \tag{8.25}$$

$$W^{imp}(i\nu_n) \stackrel{!}{=} W^{loc}(i\nu_n). \tag{8.26}$$

## 8.2 Output

After convergence, *e.g.* the local spectral function $A_m(\omega)$ can be obtained by analytic continuation of $G^{loc}_{mm}(i\omega_n)$.

## 8.3 High-frequency correction for K($\tau$)

When calculating the functions $K(\tau), K'(\tau)$, the infinite sum over bosonic Matsubara frequencies $\nu_n$ has to be properly treated.

In order to evaluate the high frequency correction terms analytically, we use the result from Cvijović and Klinowski, Proc. Amer. Math. Soc. 123, (1995):

$$\frac{\pi^{2k-1}}{(-1)^k 2(2k-1)!} B_{2k-1}(x) = \sum_{n=1}^{\infty} \frac{\sin(2n\pi x)}{(2n)^{2k-1}} \tag{8.27}$$

$$\frac{\pi^{2k}}{(-1)^{k-1} 2(2k)!} B_{2k}(x) = \sum_{n=1}^{\infty} \frac{\cos(2n\pi x)}{(2n)^{2k}}, \tag{8.28}$$

where $x \in (0,1)$ and $E_k(x)$ are the Bernoulli polynomials, with the first given as

$$B_0(x) = 1 \tag{8.29}$$

$$B_1(x) = x - \frac{1}{2} \tag{8.30}$$

$$B_2(x) = x^2 - x + \frac{1}{6} \tag{8.31}$$

With this, we can evaluate the following sums

$$\frac{1}{\beta}\sum_{n=1}^{\infty}\frac{\cos(\nu_n\tau)}{\nu_n^2} = \frac{\beta}{\pi^2}\sum_{n=1}^{\infty}\frac{\cos(2n\pi\tau/\beta)}{(2n)^2} \tag{8.32}$$

$$= \frac{\beta}{\pi^2}\frac{\pi^2}{(-1)^{1-1}2(2)!}B_2(\tau/\beta) \tag{8.33}$$

$$= \frac{1}{4\beta}\left(\tau^2 - \tau\beta + \frac{\beta^2}{6}\right) \tag{8.34}$$

$$\tag{8.35}$$

$$\frac{1}{\beta}\sum_{n=1}^{\infty}\frac{\sin(\nu_n\tau)}{\nu_n} = \frac{1}{\pi}\sum_{n=1}^{\infty}\frac{\sin(2n\pi\tau/\beta)}{2n} \tag{8.36}$$

$$= \frac{1}{\pi}\frac{\pi^{2-1}}{(-1)^1 2(2-1)!}B_{2-1}(\tau/\beta) \tag{8.37}$$

$$= -\frac{1}{2\beta}\left(\tau - \frac{\beta}{2}\right) \tag{8.38}$$

Furthermore, we also will need

$$\frac{1}{\beta}\sum_{n=1}^{\infty}\frac{1}{\nu_n^2} = \frac{\beta}{\pi^2}\sum_{n=1}^{\infty}\frac{1}{(2n)^2} \tag{8.39}$$

$$= \frac{\beta}{24} \tag{8.40}$$

Now we can apply these results to obtain analytic expressions for the high frequency tails in $K(\tau), K'(\tau)$. For large frequencies, since $\mathcal{U}(i\nu_n)$ is real and even , we can approximate $\mathcal{U}(i\nu_n)$ as

$$\mathcal{U}(i\nu_n) \approx \mathcal{V} - \frac{c}{\nu_n^2}, \tag{8.41}$$

where

$$\mathcal{V} = \lim_{\nu_n\to\infty}\mathcal{U}(i\nu_n) = \frac{1}{N_q}\sum_q V_q. \tag{8.42}$$

Assume we use $N_\nu$ bosonic frequencies in the calculation, the summation for $K(\tau)$

is split as

$$K(\tau) = -\frac{2}{\beta}\sum_{n>0}\frac{\mathcal{U}(i\nu_n)-\mathcal{U}(0)}{\nu_n^2}(\cos(\nu_n\tau)-1) \tag{8.43}$$

$$\approx -\frac{2}{\beta}\sum_{n=1}^{N_\nu-1}\frac{\mathcal{U}(i\nu_n)-\mathcal{U}(0)}{\nu_n^2}(\cos(\nu_n\tau)-1)$$

$$-\frac{2}{\beta}\sum_{n=N_\nu}^{\infty}\frac{\mathcal{V}-\frac{c}{\nu_n^2}-\mathcal{U}(0)}{\nu_n^2}(\cos(\nu_n\tau)-1) \tag{8.44}$$

$$= -\frac{2}{\beta}\sum_{n=1}^{N_\nu-1}\frac{\mathcal{U}(i\nu_n)-\mathcal{V}+\frac{c}{\nu_n^2}}{\nu_n^2}(\cos(\nu_n\tau)-1)$$

$$-\frac{2}{\beta}\sum_{n=1}^{\infty}\frac{\mathcal{V}-\frac{c}{\nu_n^2}-\mathcal{U}(0)}{\nu_n^2}(\cos(\nu_n\tau)-1) \tag{8.45}$$

This becomes too long, and either way all terms fall off quite quickly. Therefore, for now we just approximate $U(i\nu_n)\approx\mathcal{V}$ for large $\nu_n$. THis should be rechecked later.

$$-\frac{2}{\beta}\sum_{n=1}^{\infty}\frac{\mathcal{V}-\mathcal{U}(0)}{\nu_n^2}(\cos(\nu_n\tau)-1)$$

$$= -\frac{2}{\beta}\sum_{n=1}^{\infty}\left([\mathcal{V}-\mathcal{U}(0)]\frac{\cos(\nu_n\tau)}{\nu_n^2}-\frac{\mathcal{V}-\mathcal{U}(0)}{\nu_n^2}\right) \tag{8.46}$$

$$= \frac{\tau(\beta-\tau)}{2\beta}[\mathcal{V}-\mathcal{U}(0)] \tag{8.47}$$

(Final summary will be below)
For $K'(\tau)$ we proceed in the same way

$$K'(\tau) = \frac{2}{\beta}\sum_{n>0}\frac{\mathcal{U}(i\nu_n)-\mathcal{U}(0)}{\nu_n}\sin(\nu_n\tau) \tag{8.48}$$

$$= \frac{2}{\beta}\sum_{n=1}^{N_\nu-1}\frac{\mathcal{U}(i\nu_n)-\mathcal{V}}{\nu_n}\sin(\nu_n\tau)$$

$$+\frac{2}{\beta}\sum_{n=1}^{\infty}\frac{\mathcal{V}-\mathcal{U}(0)}{\nu_n}\sin(\nu_n\tau) \tag{8.49}$$

The last term evaluates as

$$\frac{2}{\beta}\sum_{n=1}^{\infty}\frac{\mathcal{V}-\mathcal{U}(0)}{\nu_n}\sin(\nu_n\tau) = \frac{2}{\beta}\sum_{n=1}^{\infty}\left([\mathcal{V}-\mathcal{U}(0)]\frac{\sin(\nu_n\tau)}{\nu_n}\right) \tag{8.50}$$

$$= 2\left([\mathcal{V}-\mathcal{U}(0)]\frac{-1}{2\beta}\left(\tau-\frac{\beta}{2}\right)\right) \tag{8.51}$$

$$= \frac{\beta-2\tau}{2\beta}[\mathcal{V}-\mathcal{U}(0)] \tag{8.52}$$

Summarizing, we obtain for the high frequency-corrected formulas for $K(\tau), K'(\tau)$ the following expressions, that are implemented in the code

$$K(\tau) = -\frac{2}{\beta}\sum_{n=1}^{N_\nu - 1}\left(\mathcal{U}(i\nu_n) - \mathcal{V}\right)\frac{\cos(\nu_n\tau) - 1}{\nu_n^2} + \frac{\tau(\beta-\tau)}{2\beta}\left[\mathcal{V} - \mathcal{U}(0)\right] \tag{8.53}$$

$$K'(\tau) = \frac{2}{\beta}\sum_{n=1}^{N_\nu - 1}\left(\mathcal{U}(i\nu_n) - \mathcal{V}\right)\frac{\sin(\nu_n\tau)}{\nu_n} + \frac{\beta-2\tau}{2\beta}\left[\mathcal{V} - \mathcal{U}(0)\right] \tag{8.54}$$

Differentiating $K(\tau)$ w.r.t. $\tau$ indeed gives the correct expression for $K(\tau')$ (would have saved a lot of work...) REMEBER: These formulas are derived for $\tau \in (0, \beta)$! The Alps solver requires $K(\tau)$ to be positive and $K(0) = 0$, which is fulfilled in this form.

For the solver we need to provide the instantaneous $U_{ij}$ values in `u_matrix.dat`, which means we have to use the bare $\sim \mathcal{V}$ values. The local chemical potential is written in `mu_vector.dat`. All necessary shifts that need to be done for the solver, like $U_{ij} \to U_{ij} + 2K'(0)$ and $\mu \to +K'(0)$ is this the right sign are done in the ALPS solver, so we do not need to worry about this.

## 8.4 High-frequency terms for $G_{bath}$ and Hybridization fucntion, local $\mu$

One of the slowest decaying functions on the Matsubara axis are actually the bath Green's function $\mathscr{G}(i\omega_n)$, it's inverse and the hybridization function $\Delta(i\omega_n)$. The reason is that $\mathscr{G}(i\omega_n)$ is the interacting Green's function without the Hartree term, which means it's spectral weight is mostly located at binding energies close to the Hartree energy, which becomes increasingly large for frequency dependent interactions.

Since $\Delta(i\omega_n)$ is a linear function of $\mathscr{G}^{-1}(i\omega_n)$, the same holds for the hybridization function. Therefore, the determination of for example the local chemical potential as

$$\mu_{loc} = \lim_{\omega_n \to \infty} \mathrm{Re}\mathscr{G}^{-1}(i\omega_n), \tag{8.55}$$

becomes increasingly difficult.

Using the Dyson equation we can calculate this term from the coefficients of the Selfenergy and local Green's function, which decay much faster

$$\mathrm{Re}\mathscr{G}^{-1}(i\omega_n) = \mathrm{Re}G_{loc}^{-1}(i\omega_n) + \mathrm{Re}\Sigma(i\omega_n). \tag{8.56}$$

Keeping terms only up to $\mathcal{O}(1/\omega_n^4)$, at large frequencies the terms can be approxi-

mated as

$$\mathrm{Re}G_{loc}^{-1}(i\omega_n) + \mathrm{Re}\Sigma(i\omega_n) = \frac{\mathrm{Re}G_{loc}(i\omega_n)}{\mathrm{Re}G_{loc}(i\omega_n)^2 + \mathrm{Im}G_{loc}(i\omega_n)^2} + \mathrm{Re}\Sigma(i\omega_n) \tag{8.57}$$

$$\approx \frac{\frac{-g_2}{\omega_n^2} + \frac{g_4}{\omega_n^4}}{\left[\frac{-g_2}{\omega_n^2} + \frac{g_4}{\omega_n^4}\right]^2 + \left[\frac{-g_1}{\omega_n} + \frac{g_3}{\omega_n^3}\right]^2} + \Sigma_0 + \frac{-\Sigma_2}{\omega_n^2} \tag{8.58}$$

$$\approx \frac{\frac{-g_2}{\omega_n^2} + \frac{g_4}{\omega_n^4}}{\frac{g_2^2}{\omega_n^4} + \frac{g_1^2}{\omega_n^2} + \frac{-2g_1g_3}{\omega_n^4}} + \Sigma_0 - \frac{\Sigma_2}{\omega_n^2} \tag{8.59}$$

$$= \frac{-g_2 + \frac{g_4}{\omega_n^2}}{\frac{g_2^2}{\omega_n^2} + g_1^2 - \frac{2g_1g_3}{\omega_n^2}} + \Sigma_0 - \frac{\Sigma_2}{\omega_n^2} \tag{8.60}$$

$$= \Sigma_0 + \frac{-g_2}{g_1^2 + \frac{g_2^2 - 2g_1g_3}{\omega_n^2}} + \frac{1}{\omega_n^2}\frac{g_4}{g_1^2 + \frac{g_2^2-2g_1g_3}{\omega_n^2}} - \frac{\Sigma_2}{\omega_n^2} \tag{8.61}$$

$$\approx \Sigma_0 - g_2/g_1^2 + \mathcal{O}(1/\omega_n^2) \tag{8.62}$$

Since for a usual Green's function $g_1 = 1$, we usually have

$$\mathrm{Re}\mathscr{G}^{-1}\omega_n \approx \Sigma_0 - g_2 + \mathcal{O}(1/\omega_n^2) \tag{8.63}$$

and therefore

$$\mu_{loc} = \Sigma_0 - g_2 \tag{8.64}$$

# 9 Analytic continuation

The analytic continuation becomes increasingly hard for the case of frequency dependent interactions $U(\omega)$, since plasmonic features appear in the spectral function, resp. Green's function at multiples of the plasma frequency, for example in $SrVO_3$ $\omega_p \approx 15$ eV. Therefore, the energy window has to be chosen considerably large, at least $\pm 3\omega_p$ to obtain a proper normalization of the spectral function.

At the same time the high-energy features cannot be accurately resolved because the kernel that has to be inverted becomes very small at high energies

$$G(i\omega_n) = \frac{1}{\pi}\int_{-\infty}^{\infty} \mathrm{Im}[G(\omega)]\frac{1}{\omega - i\omega_n}\mathrm{d}\omega \tag{9.1}$$

$$G(\tau) = \frac{1}{\pi}\int_{-\infty}^{\infty} \mathrm{Im}[G(\omega)]\frac{\mathrm{e}^{-\tau\omega}}{\mathrm{e}^{-\beta\omega}+1}\mathrm{d}\omega. \tag{9.2}$$

Performing the analytic continuation from the Matsubara axis $i\omega_n$ should in principle be easier, since the Kernel $K(\omega, i\omega_n) = \frac{1}{\omega - i\omega_n}$ does decay significantly slower than the Kernel $K(\omega,\tau) = \frac{\mathrm{e}^{-\tau\omega}}{\mathrm{e}^{-\beta\omega}+1}$ for the continuation to the imaginary time axis $\tau$. Therefore, plasmonic features at large $\omega$ are less suppressed by $K(\omega, i\omega_n)$ than by $K(\omega,\tau)$, so small changes on the real frequency axis $\omega$ should be more visible in $G(i\omega_n)$ than in $G(\tau)$.

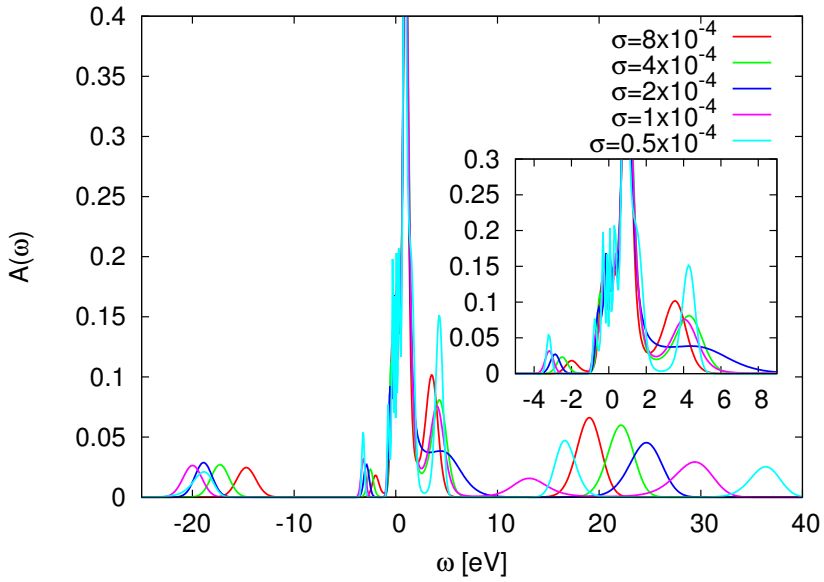


Figure 3: The spectral function from $G_0W_0$ (7x7x7 k-points) obtained from Maxent, using a constant standard deviation $\sigma$. The Green's function on the Matsubara axis $i\omega_n$ for 1000 frequenices at $\beta = 40$ 1/eV was continued using a gaussian default model.

In practice I think it is still better to use Maxent with $G(\tau)$ directly measured at $\tau_i$, since the Legendre representation usually used on both $\tau$ and $i\omega_n$ introduces very spurious correlated errors in the measured quantities, where no good error estimate exist. Only for $G(\tau)$ we have a well defined measure of the error bar which is measured in the solver and should be used for the Maxent input. Maybe one can use the direct measurement on $i\omega_n$ (more costly) in the future?

**Essential tip:** A very efficient way of dealing with the plasmonic weight at high frequencies is by incorporating them already in the default model. What works quite well is adding gaussians at multiple of the plasma frequency $\pm n\omega_0$, with $n \sim 4$, that become smaller in weight. Usually, the positions of these gaussians will not be modified becuase the analytic continuation is not sensitive enough to determine their correct position but they are essential for redistributing spectral weight away from the Fermi level. Another option is to add, instead of gaussians, only a constant value, which reaches up to high energies. The important point here is that the spectral weight at the Fermi level, which is usually a bigger gaussian in the default model, is properly reduced so that the analytic continuation does not have to shift spectral weight from the Fermi level over long distances to higher energies.

With both of these models, I noticed that the resulting spectral function around the Fermi level is only very weakly dependent on the choice of $\sigma$, which makes the result very robust and trustworthy. Also the position of the (first) upper and lower Hubbard bands seem to be quite robust. On both the imaginary time and frequency axis it worked quite well and gave very similar results.

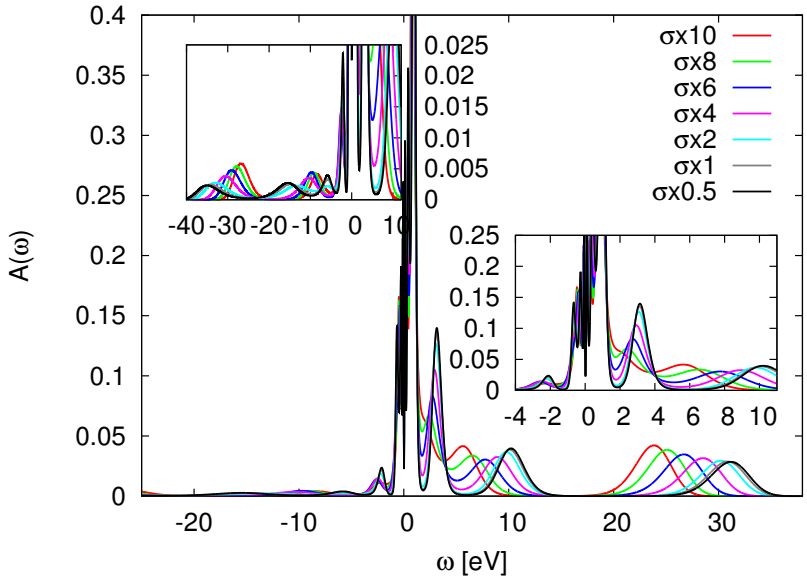


Figure 4: The spectral function from GW+DMFT (7x7x7 k-points) obtained from Maxent, using the mesured standard deviation $\sigma(\tau)$ from the impurity solver. The Green's function on the imaginary time axis $\tau$ for 2048 points at $\beta = 40$ 1/eV was continued using a gaussian default model. The standard deviation was scaled by different factors to show the dependence on $\sigma$. The factor 1 corresponds to the initial value of $\sigma$ measured in the Monte Carlo Solver.

# 10 Dependence on the k-mesh

This section discusses the sensitivity of the GW calculation on the number of k-points. There are three quantities of interest:
The Kohn-Sham DFT Hamiltonian $H_{DFT}$, the exchange-correlation potential $V_{XC}$ and the GW Selfenergy $\Sigma_{XC}^{GW}$. All of them are given in the Basis of Wannier orbitals.

In general the GW calculation is limited to k-meshes with a size from $5 \times 5 \times 5$ to maximum $10 \times 10 \times 10$, depending on how large the system is. Currently the limitation of the GW calculation is the memory and disk space. For example a $8 \times 8 \times 8$ calculation for $SrVO_3$ exceeds the 128Gbyte RAM on a single node on Hedin and uses more than 1Tbyte of disk space. The computation time is still manageable with less than one week.

After the GW calculation the result is interpolated to a very dense k-mesh by a 3D cubic interpolation scheme, which so far has been very reliable.

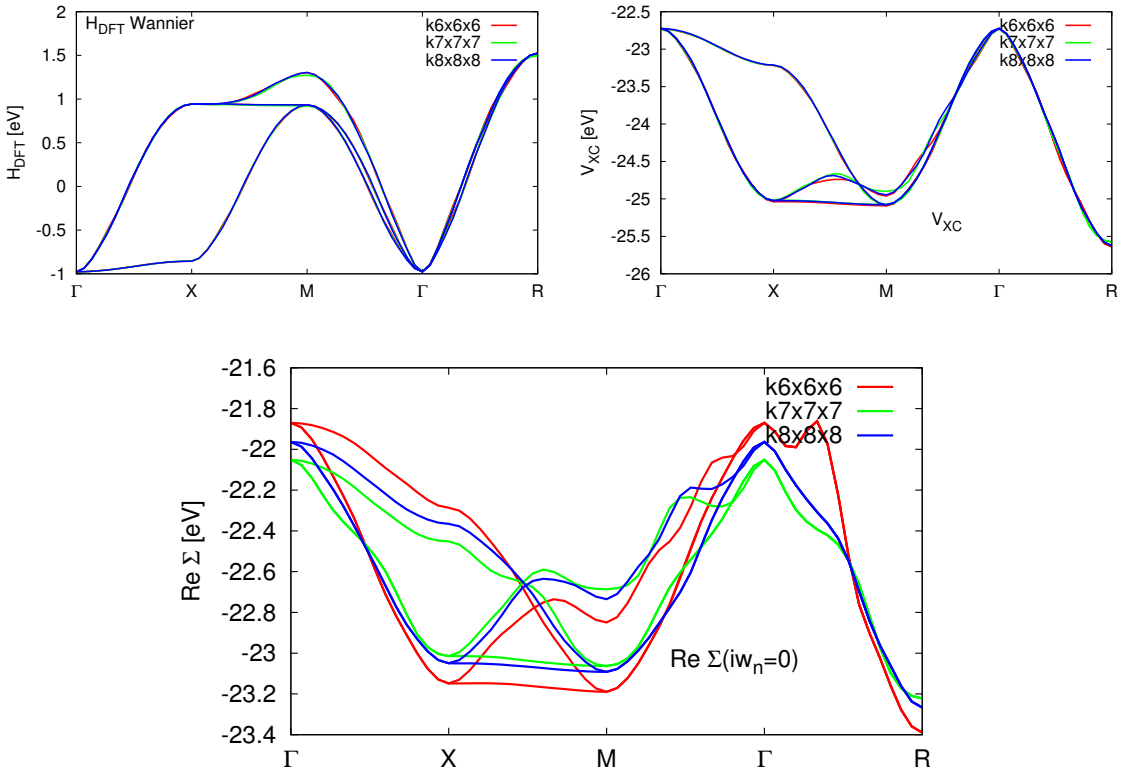


Figure 5: These plots show a comparison of the convergence of $H_{DFT}$, $V_{XC}$ and $\Sigma_{XC}^{GW}$ in the Wannier basis as a function of number of k-points for $SrVO_3$.
Top Left: The Eigenvalues of the DFT tight-binding Hamiltonian $H_{DFT}$.
Top Right: The exchange-correlation potential $V_{XC}$.
Bottom: The real part of the **local** $G_0W_0$ Selfenergy, which is equal for all 3 $t_{2g}$ orbitals, evaluated at the lowest Matsubara frequency ($\beta = 40$ 1/eV).

## 10.1 $SrVO_3$

In Fig. 5 we show the Eigenvalues of the DFT tight-binding Hamiltonian $H_{DFT}$, the exchange-correlation potential $V_{XC}$ and the real part of the $G_0W_0$ Selfenergy at the lowest Matsubara frequency at $\beta = 40$ 1/eV along a certain k-path. Calculations based on different k-meshes in the GW calculation are compared. All objects have been interpolated to a $30 \times 30 \times 30$ k-mesh.

$H_{DFT}$ shows basically negligible variation for different number of k-points since the values are directly taken from the DFT calculation converged on a much denser grid. The only variation is due to the interpolation from the smaller to the larger grid, which becomes more accurate with higher number of k-points.

Interestingly, $V_{XC}$ shows a much larger variation than $H_{DFT}$, for example of up to 50 meV along the X-M direction. Since for all calculations $V_{XC}$ in the Kohn-Sham space is identical, this indicates that $V_{XC}$ is either more difficult to interpolate because it is less smooth than $H_{DFT}$, or that it is itself more sensitive to the accuracy of the Wannier orbitals, which becomes more accurate with larger k-meshes.

The GW Selfenergy $\Sigma_{XC}^{GW}$ shows a really strong variation with different k-meshes and still changes more than 100meV at some k-points when increasing the mesh from $7 \times 7 \times 7$ to $8 \times 8 \times 8$. These changes of the "bandwidth" that can be seen in the plot directly amount to a different renormalization due to the GW selfenergy, which will later have an effect on the GW+DMFT cycle.

**Plan: I think I would be satisfied with a $9 \times 9 \times 9$ calculation. This might be possible if I can get ∼900 cores on Hedin for maybe a week...**

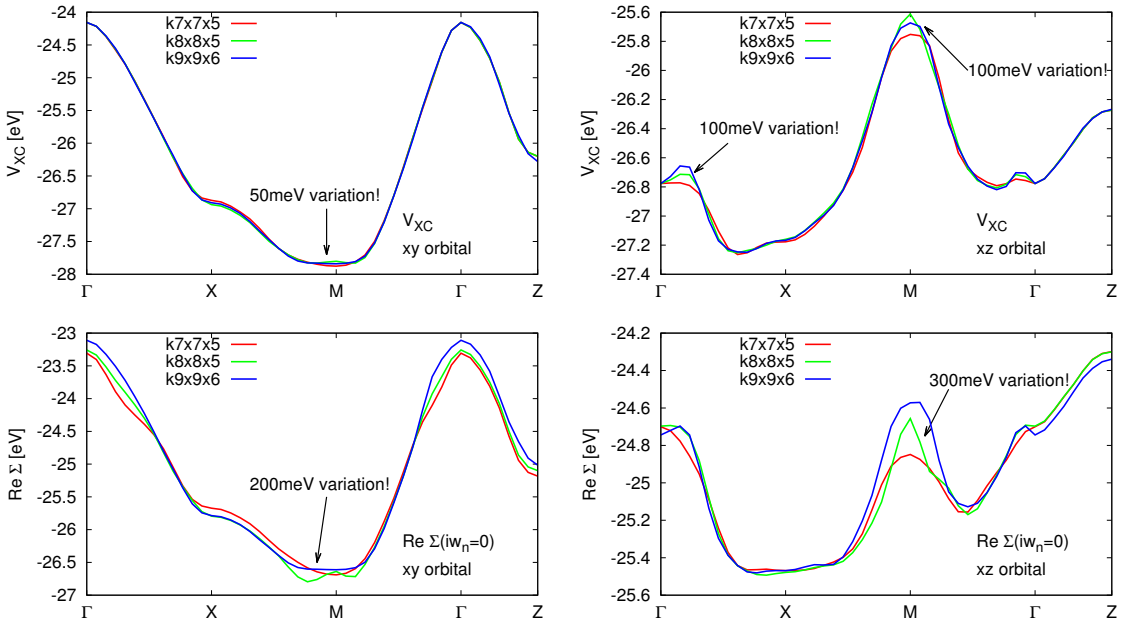


Figure 6: Top: The exchange-correlation potential $V_{XC}$ for the 3dxy and 3dxz orbital for FeSe
Bottom: The real part of the $G_0W_0$ Selfenergy at the lowest Matsubara frequency for the 3dxy and 3dxz orbital.

# 11 FeSe

Here we compare the exchange correlation potential and the GW Selfenergy for FeSe. The Kohn-Sham Hamiltonian was basically identical for all k-meshes, so we do not show it here.

Fig. 6 shows $V_{XC}$ and $\Sigma_{XC}^{GW}$ again along a certain k-path. The variations are a bit larger compared to $SrVO_3$, especially around the M point one can observe artefacts. Especially the Selfenergy varies dramatically in the 3dxz orbital, with variation of about 300 meV. These variations directly translate to shifts of "bands", also around the Fermi level. This can be seen clearly when calculating the full GW spectral function, shown in Fig. 7. There are artefacts appearing basically at all high-symmetry points, but especially severe around the M point. In this case the $9 \times 9 \times 6$ mesh fixes these problems, but even this mesh cannot be considered to be converged sufficiently.

Interestingly, the calculations with odd number of k-points along each axis seem to show less artefacts, probably because the high-symmetry points are excluded and obtained only by interpolation.

**Plan: I think I would be satisfied with a $9 \times 9 \times 7$ calculation. This is currently running...**

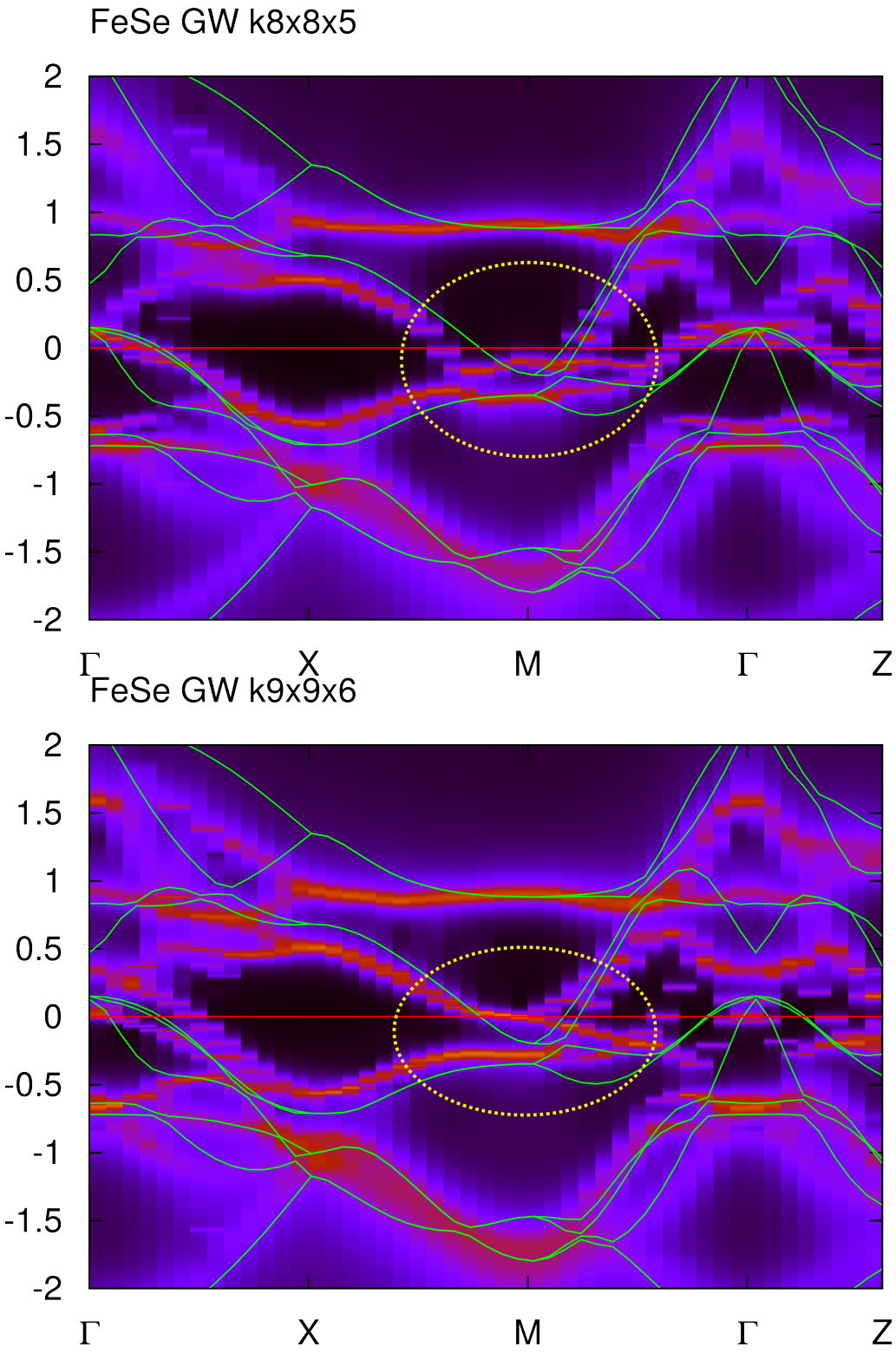


Figure 7: The spectral function of FeSe calculated within GW. Upper panel shows the result for a $8 \times 8 \times 5$ k-mesh, and the lower one for a $9 \times 9 \times 6$ k-mesh. The green lines are the DFT result. The artefacts at the M point (yellow circle) are a result of the k-mesh being still too coarse.

# 12 Dependence on GW frequency mesh

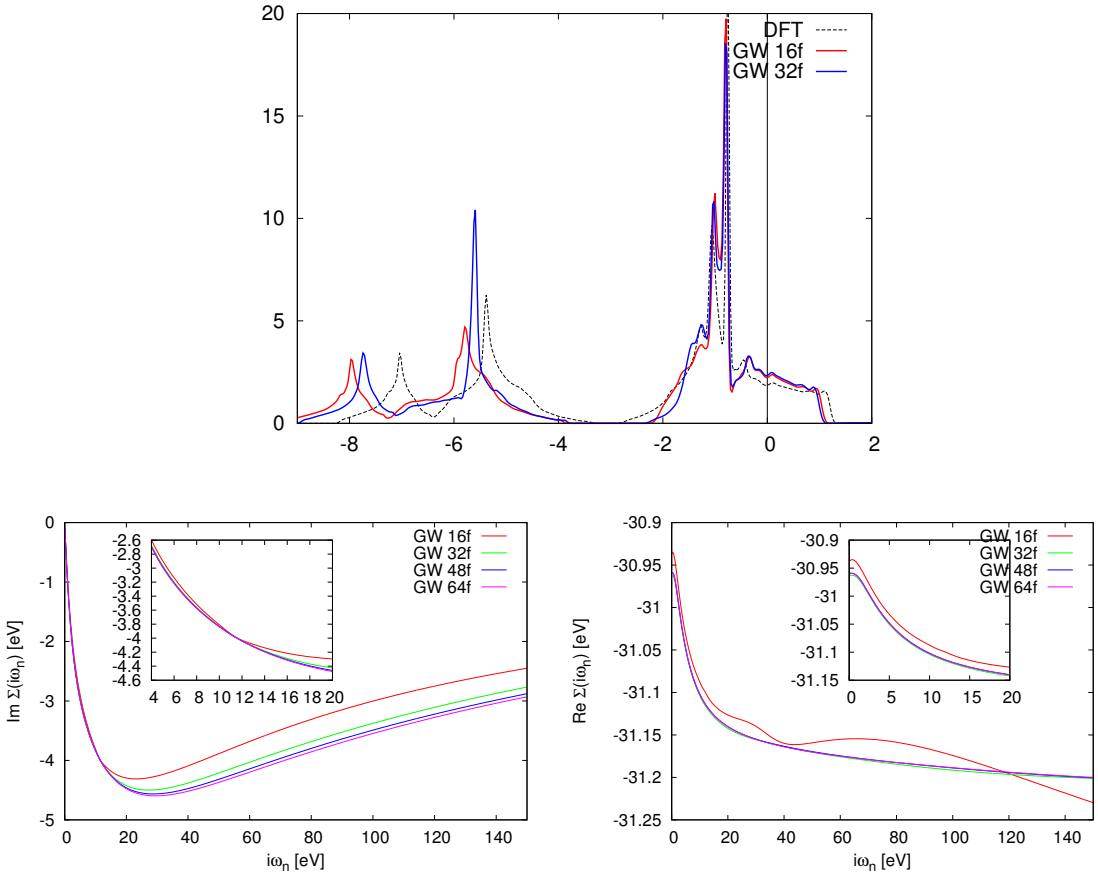


Figure 8: Top: The GW quasiparticle DOS for NiO with different number of frequenices used for sampling the Polarization/Selfenergy. Bottom: The resulting selfenergy for different number of frequencies. In the imaginary part the Selfenergy at the Gamma point for the $e_g$ orbitals is shown, while in the real part it is shown at the X point for the first $e_g$ orbital.

In the GW Code the frequency dependent objects are stored on a specific frequency mesh, which is also used for integration when evaluating the Selfenergy

$$\Sigma^{GW}(i\omega) = \int \mathrm{d}i\nu \; G(i\omega - i\nu)W(i\nu). \tag{12.1}$$

In the gw.inp input file one has the parameters

**iop_fgrid** :

- **1** Equally spaced mesh
- **2** single Gauss-Laguerre quadrature
- **3** Double Gauss-Legendre quadrature from 0 to omegmax and from omegmax to infinity
- **4** Fermion Matsubara frequencies

The default is the double Gauss-Legendre quadrature, in which the semi-infinite integral from 0 to infinity is divided into two intervals $[0, \omega_0]$ and $[\omega_0, \infty]$, and the integration in each interval is carried out by standard Gauss-Legendre quadrature. The default value for $\omega_0 = 0.42$ Hartree $\approx 11.4$ eV.

**nomeg** total number of frequencies

**omegmax** This is $\omega_0$ for GW calculations. In the case of cRPA calculations, omegmax and omegmin indicate the upper and lower bounds of the frequency grid on which the screened Coulomb interactions are calculated.

**nomeg_blk** This is a technical parameter that can be used when nomeg is very large. In that case, the memory size required can be huge and therefore the loop over the frequency can be divided into blocks with the size of nomeg_blk.

For insulators the number of frequencies does not have a big effect, but in metals like SrVO3, or NiO (metal in DFT) I noticed a very significant influence. In Fig. 8 the effect of using different number of frequencies on the GW DOS and the Selfenergy is shown. In general it seems that nomeg=16 is significantly too low, and nomeg=48 is almost enough. nomeg=64 should be sufficiently converged, but usually impossible to calculate for larger k-meshes due to memory constraints. For $SrVO_3$ I currently cannot use more that 22, and in FeSe not more than 30. The dependency in the systems I investigated (NiO, FeSe, SrVO3) is very similar, with $SrVO_3$ converging a bit faster than the other two.

I also did tests using different omegmax values but it seems the default one is quite ok, and one only needs to use as much frequencies as possible.

**Important Warning:**

In Fig. 8 in the lower right the real part of the GW Selfenergy is shown. One observes a slight oscillating behaviour for a low number of frequencies but close to the converged value. **A very severe problem** is that this Selfenergy does not have a proper high-frequency behaviour, with the high-frequency tail not decaying as $\sim c_0 + \frac{c_2}{(i\omega)^2} + ....$ This can be remedied with using more frequencies, but the problem persists even until 30 frequencies. Even though the deviation is not large, this creates a significant problem when evaluating the hybridization function $\Delta(i\omega)$

$$\Delta(i\omega) = i\omega + \mu - \mathscr{G}^{-1}_{bath}(i\omega) \tag{12.2}$$
$$= i\omega + \mu - G^{-1}_{loc}(i\omega) - \Sigma_{imp}(i\omega). \tag{12.3}$$

As discussed in more detail in the next section, we still retain effects of a term of the following form in $\Delta(i\omega)$

$$\sum_k \Sigma^{GW}(k) - \Sigma^{DC} \neq 0.$$

Now the situation is the following:
The high freqeuency tail of $\Sigma^{DC}$ is correct, because we evaluate it directly at finite temperature using all Matsubara frequencies, and not inside the GW code. On the other hand, the high freqeuency tail of $\sum_k \Sigma^{GW}(k)$ is usually not correct, if only a

small number of frequencies has been used in the GW calculation. **As a result the determination of the impurity levels**

$$\mu_{imp} = \lim_{i\omega\to\infty} \mathrm{Re}\left[G^{-1}_{loc}(i\omega) - \Sigma_{imp}(i\omega)\right]$$

**is extremely inaccurate or even becomes impossible**. The calculation of the Fourier transform $\Delta(\tau)$ needed for the impurity solver becomes inaccurate as well, since it relies on a proper high-frequency treatment of the tails of $\Delta(i\omega)$.

This can be seen clearly in Fig. 9, which shows the resulting impurity hybridization function $\Delta(i\omega_n)$ for FeSe, using different frequency grids for the calculation of the GW Selfenergy. Even for 30 frequencies the tail is too ill-behaved to perform a realiable high frequency fit. Please note that this does not depend on how many Matsubara frequencies are used in the DMFT calculation itself. If the number of $i\omega_n$ were increased, the tail in the following plot would never recover and just diverge linearly to infinity (can be seen in the red line quite clearly):

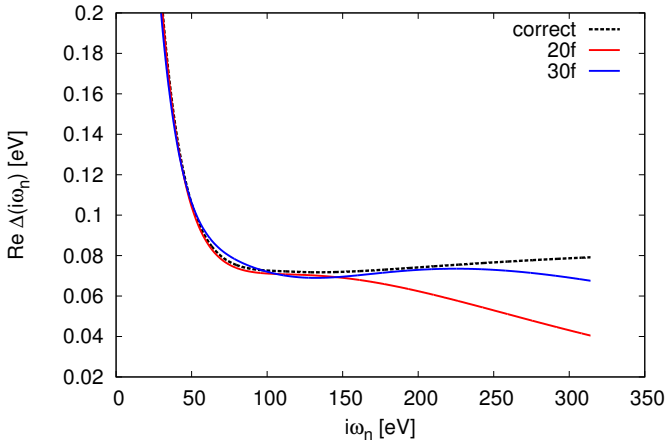


Figure 9: This plot shows the real part of the impurty hybridization function $\Delta(i\omega_n)$ for FeSe, using different frequency grids for the calculation of the GW Selfenergy. Since the tail of the GW Selfenergy is usually not well behaved, also the tail of $\Delta(i\omega_n)$ is usually wrong. For 20 frequencies the tail deviates very quickly from the correct behaviour, while for 30 frequencies the deviations sets in later, but still does not allow a proper high frequency fitting of the tail.

**Solution for now**: In principle one should increase the number of frequencies in the GW calculation, but for this we need at least 60 frequencies which is impossible right now in terms of calculation time and memory consumption. Therefore, we fit the GW Selfenergy in a frequency range which is still reliable but as large as possible with the following form

$$\mathrm{Re}\Sigma(i\omega) \sim c_0 + \frac{c_2}{(i\omega)^2} + \frac{c_4}{(i\omega)^4} \tag{12.4}$$

and replace the tail completely by this expression. In FeSe in Fig. 9 this is the case around 100 eV, where we cut all further values and replace them by the fitted

expression above. This is done for all orbital components of the GW Selfenergy at each k-point.

This of course introduces some kind of error, since around 100 eV the GW Selfenergy is not sufficiently described by such a term as the one above. Still, this is probably the better way since the high-frequency tail without this treatment would be even more wrong, and would prevent a calculation of the impurity levels and $\Delta(\tau)$, as discussed above.

# 13 Doublecounting effects on the hybridization

It is interesting to investigate the effects of the Doublecounting used in GW+DMFT on the hybridization function.

$$\Delta(i\omega) = i\omega + \mu - \mathscr{G}^{-1}_{bath}(i\omega) \tag{13.1}$$
$$= i\omega + \mu - G^{-1}_{loc}(i\omega) - \Sigma_{imp}(i\omega). \tag{13.2}$$

The hybridization function $\Delta(i\omega_n)$ effectively encodes the bath of the impurity and thus carries the information about the surrounding lattice. In standard lattice DMFT without extensions this bath is purely noninteracting and just given by the free lattice dispersion.

In LDA+DMFT, since we perform a downfolding from the full space to a low-energy subspace, where the bath now encodes all information about the outer space, the bath is no longer non-interacting. It contains all interaction effects residing in the outer space on the DFT level. Thus, which is an important point!, purely on a one-particle level, i.e. the hybridization function can still be written like a non-interacting lattice hybridization

$$\Delta(i\omega) = \sum_{kj} \frac{|V^j_k|^2}{i\omega_n - \epsilon^j_k} \tag{13.3}$$

From the definition $\Delta(i\omega) = i\omega + \mu - G^{-1}_{loc}(i\omega) - \Sigma_{imp}(i\omega)$ I think it makes sense that $\Delta(i\omega)$ can also encode an interacting bath, that contains interactions in the outer space, since it is basically the local lattice Green's function minus the local interactions. **(But I need to go through the DMFT derivation again...)**

In GW+DMFT the hybridization or resp. the bath can become even "more interacting", depending on what kind of doublecounting we use:

- If the full local GW Selfenergy is subtracted as the doublecounting

  $$\Sigma^{DC} = [GW]_{loc}\,,$$

  then basically also all the local Selfenergy effects in $G_{loc}$ are originating purely from $\Sigma_{imp}$, since

  $$G(k, i\omega_n) = \big[\mathbb{1}(i\omega_n + \mu) - H^{DFT}(k) + v^{XC}(k) - \Sigma^{GW}(k, i\omega_n) + \Sigma^{DC}(i\omega_n) - \Sigma^{imp}(i\omega_n)\big]^{-1} \tag{13.4}$$

This part is then subtracted when creating $\Delta(i\omega)$, thus there is effectively no remainder of a local Selfenergy in $\Delta(i\omega)$. This usually gives a fast decaying high-frequency tail of $\Delta(i\omega)$.

- If only the impurity contribution is subtracted from GW

$$\Sigma^{DC} = G_{loc}W_{loc},$$

then the local Selfenergy effects in $G_{loc}$ are originating not only from $\Sigma_{imp}$ BUT there is also a contribution from GW since

$$\sum_k \Sigma^{GW}(k) - \Sigma^{DC} \neq 0,$$

that stems from the contributions of nonlocal propagators to the local Selfenergy, that are not captured by DMFT. As an example we compare the local GW Selfenergy, the Doublecounting term and the remaining component in Fig. 10 for $SrVO_3$:

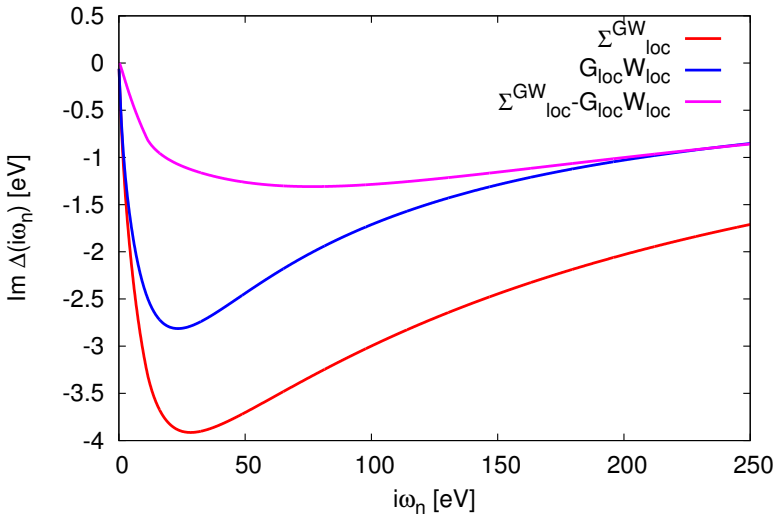


Figure 10: This plot shows the local GW Selfenergy (averaged over k-points) in comparison to the $G_{loc}W_{loc}$ doublecounting, which only includes the GW contribution on the impurity, and therefore is smaller than the local GW part. The difference between the two (pink line) is what remains in the local GW Selfenergy from non-local propagators. It is still comparable in size to the GW Selfenergy and decays similarly slow, so still contains many high-energies features.

This has the effect that now there is effectively a remainder of a local GW Selfenergy in $\Delta(i\omega)$. This leads to very slowly decaying high-frequency tail of $\Delta(i\omega)$, since the remaining Selfenergy still creates features plasmonic-like features at higher energy, which are now encoded in the effective DMFT bath.

Now the hybridization function can no longer be written like a non-interacting lattice hybridization

$$\Delta(i\omega) = \sum_{kj} \frac{|V_k^j|^2}{i\omega_n - \epsilon_k^j} \tag{13.5}$$

But I think this is also the case for the other doublecounting? Since it contains nonlocal components of the GW Selfenergy?... But here in this case the bath carries information about a local Selfenergy that also resides on the impurity, but cannot be generated from only the local interactions on the impurity!! The meaning is not clear to me yet...

As an example we show the hybridization function for $SrVO_3$ in Fig. 11 calculated from a GW+DMFT calculation with the two different doublecountings. We immediately see that the energy scales of the impurity bath are different by orders of magnitude.

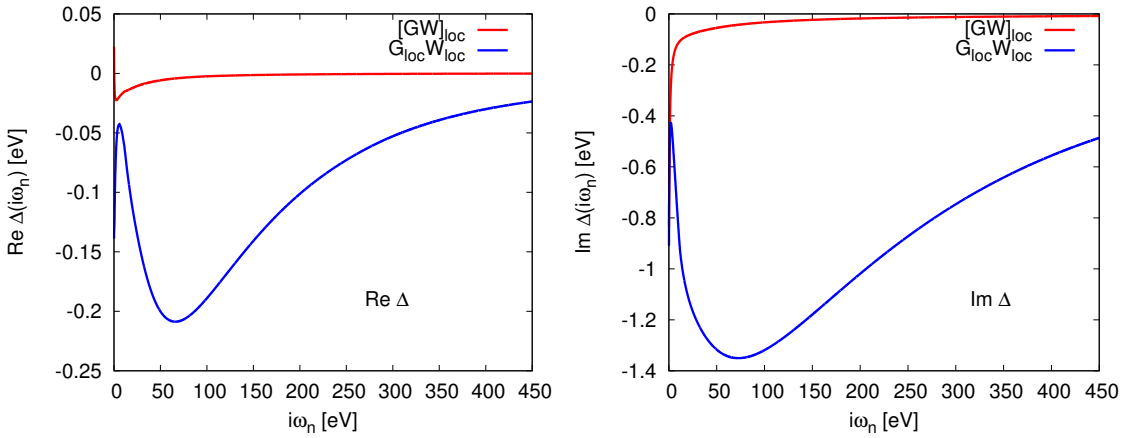


Figure 11: This plot shows the impurty hybridization function $\Delta(i\omega_n)$ for $SrVO_3$, for the two different types of doublecounting that we use. For the $[GW]_{loc}$ Doublecounting, the full local part of the GW Selfenergy is substracted, while for the $G_{loc}W_{loc}$ Doublecounting only the impurity GW contribution is subtracted. Therefore, there is a local Selfenergy component remaining in the hybridization function, giving rise to high energy features in the bath, that can be identified as very slowly decaying tails in $\Delta(i\omega_n)$.

# 14 Preliminary GW+DMFT results

## 14.1 $SrVO_3$

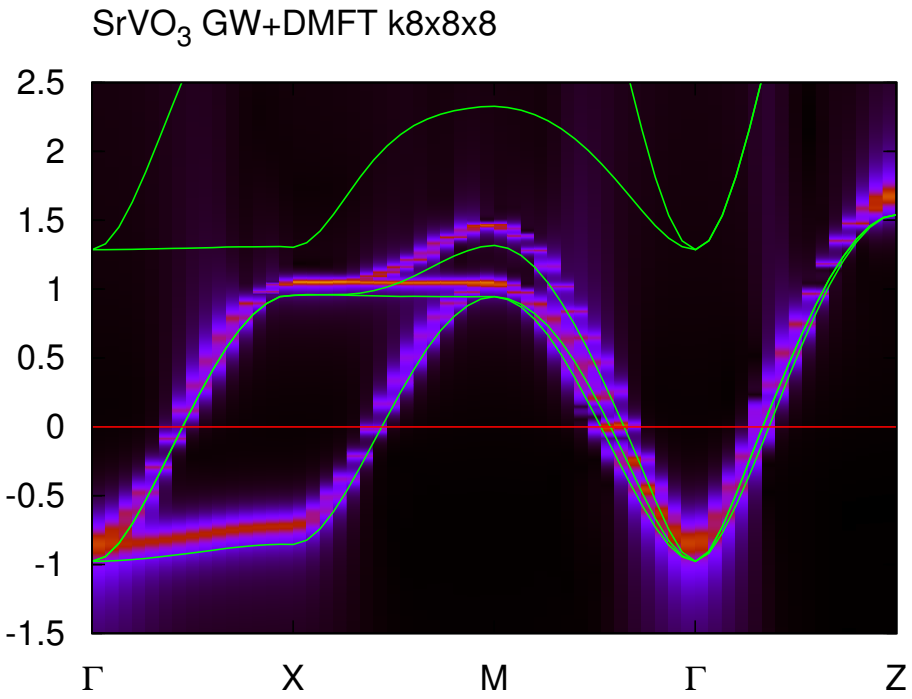


Figure 12: The spectral function for $SrVO_3$ within GW+DMFT with the $G_{loc}W_{loc}$ doublecounting. The green lines show the DFT dispersion

## 14.2 FeSe

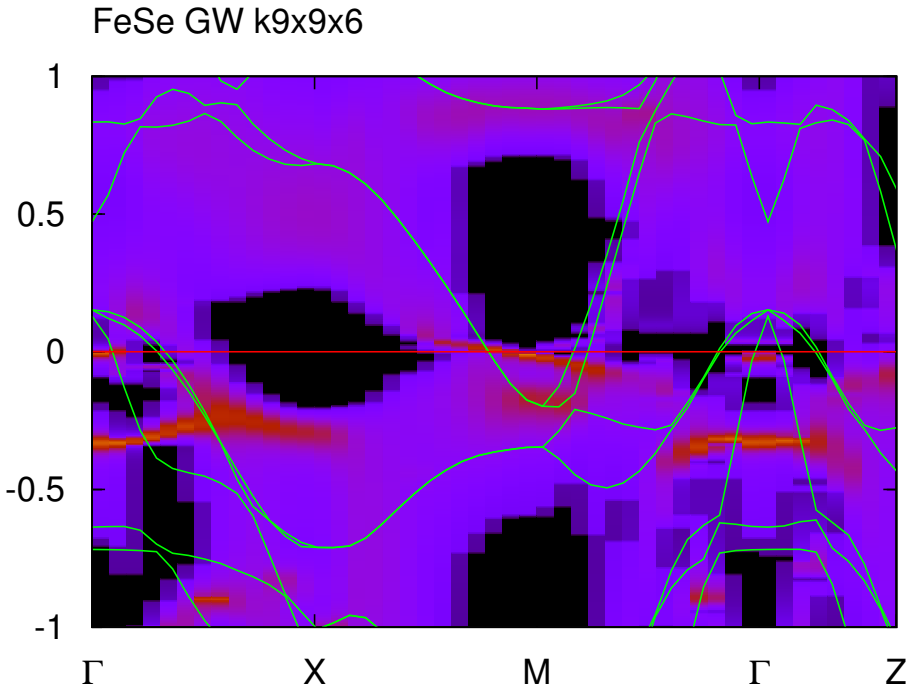


Figure 13: The spectral function for FeSe within GW+DMFT with the $G_{loc}W_{loc}$ doublecounting. The green lines show the DFT dispersion

## 14.3 NiO

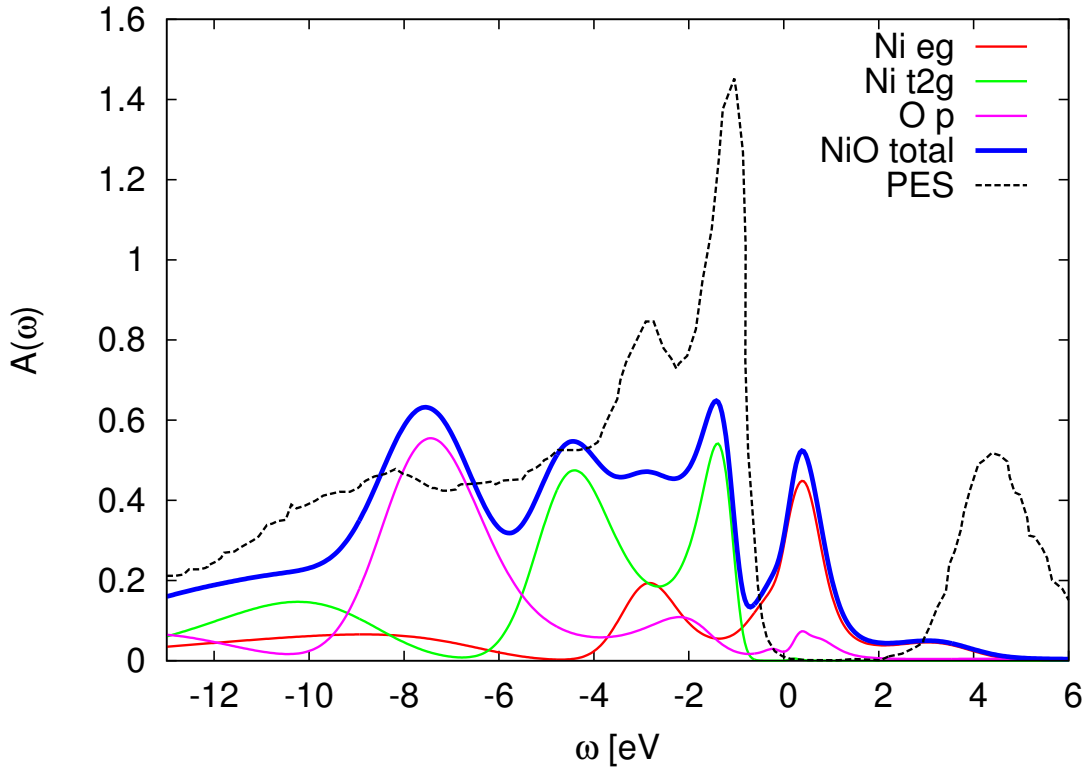


Figure 14: The local spectral function for NiO within GW+DMFT, using a dp model, compared to PES experiment.

Well, this doesn't look so bad for the first try of doing GW+DMFT for a d-p model. Unfortunately the eg's are not insulating...

# 15 Causality constraint

**Definition:** A Green's function $G$, Selfenergy $\Sigma$, or other functions $F$ derived from them is called *causal*, if

$$\mathrm{Im}F(\omega) \leq 0 \ \forall \omega \in \mathbb{R}. \tag{15.1}$$

Does it have to be strictly negative? For example, if a Green's function is causal then its related spectral function $A(\omega) = -\mathrm{Im}G(\omega)/\pi \geq 0$.

**Theorem:** A function $F(\omega)$ is causal if and only if its corresponding transform $F(\tau)$ to the imaginary time interval $(0, \beta)$ has only negative definite even derivatives, i.e.

$$F(\omega) \text{ causal } \Leftrightarrow \frac{\partial^{2n}}{\partial \tau^{2n}} F(\tau) \leq 0 \ \forall n \in \mathbb{N}. \tag{15.2}$$

Maybe its strictly negative?

**Proof:**

$\Rightarrow$: Assume that $\mathrm{Im}F(\omega) \leq 0 \ \forall \omega \in \mathbb{R}$. Using Cauchy's integral formula we have the relation

$$F(i\omega_n) = \frac{1}{\pi} \int_{-\infty}^{\infty} \frac{\mathrm{Im}F(\omega)}{\omega - i\omega_n} \, \mathrm{d}\omega \tag{15.3}$$

$$F(\tau) = \frac{1}{\pi} \int_{-\infty}^{\infty} \mathrm{Im}F(\omega) \frac{\mathrm{e}^{-\tau\omega}}{\mathrm{e}^{-\beta\omega} + 1} \, \mathrm{d}\omega \tag{15.4}$$

The Kernel in the second expression $K(\tau, \omega) = \mathrm{e}^{-\tau\omega} / \left(\mathrm{e}^{-\beta\omega} + 1\right)$ is strictly positive and decays exponentially for large $|\omega|$ for fixed $\tau \in (0, \beta)$

$$\lim_{\omega \to \infty} \frac{\mathrm{e}^{-\tau\omega}}{\mathrm{e}^{-\beta\omega} + 1} = \lim_{\omega \to \infty} \frac{\mathrm{e}^{-\tau\omega}}{0 + 1} \tag{15.5}$$

$$= 0 \tag{15.6}$$

$$\lim_{\omega \to -\infty} \frac{\mathrm{e}^{-\tau\omega}}{\mathrm{e}^{-\beta\omega} + 1} = \lim_{\omega \to -\infty} \frac{\mathrm{e}^{-\tau\omega}}{\mathrm{e}^{-\beta\omega}} \tag{15.7}$$

$$= \lim_{\omega \to -\infty} \mathrm{e}^{(\beta - \tau)\omega} \tag{15.8}$$

$$= 0. \tag{15.9}$$

In the limits $\tau = 0$ or $\tau = \beta$ the Kernel $K(\tau, \omega)$ becomes the Fermi distribution function for either negative or positive $\omega$

$$\lim_{\tau \to 0} \frac{\mathrm{e}^{-\tau\omega}}{\mathrm{e}^{-\beta\omega} + 1} = \frac{1}{\mathrm{e}^{\beta(-\omega)} + 1} \tag{15.10}$$

$$\lim_{\tau \to \beta} \frac{\mathrm{e}^{-\tau\omega}}{\mathrm{e}^{-\beta\omega} + 1} = \frac{\mathrm{e}^{-\beta\omega}}{\mathrm{e}^{-\beta\omega} + 1} \tag{15.11}$$

$$= \frac{1}{\mathrm{e}^{\beta\omega} + 1} \tag{15.12}$$

For the derivatives $\partial_\tau^{2n} F(\tau)$ we get the expression

$$\frac{\partial^{2n}}{\partial\tau^{2n}} F(\tau) = \frac{1}{\pi}\int_{-\infty}^{\infty} \mathrm{Im}F(\omega) \frac{\partial^{2n}}{\partial\tau^{2n}} \frac{\mathrm{e}^{-\tau\omega}}{\mathrm{e}^{-\beta\omega}+1}\,\mathrm{d}\omega \tag{15.13}$$

$$= \frac{1}{\pi}\int_{-\infty}^{\infty} \mathrm{Im}F(\omega)\omega^{2n} K(\tau,\omega)\,\mathrm{d}\omega. \tag{15.14}$$

Since $\mathrm{Im}F(\omega) \leq 0\ \forall\omega \in \mathbb{R}$, the integral is also strictly non-positive.

$\Leftarrow$:

Do not investigate further since: Using this for analytic continuation does not work since any least-square fitting even without enforcing the derivative constraints is too ill-behaved.

# 16 Implementation details

## 16.1 Impurity solver input

The CT-HYB impurity solver by Yusuke needs the following input files

**dmft.input** Includes information about U,J, number of frequencies, etc. At the moment possible: Only 3-fold degenerate orbitals. No freq. dependent U.

**hyb_tau.dat** The hybridization function as a matrix for imaginary time. It needs to be diagonal!
Only real part, one column. Seperate matrix elements via two line breaks and `# hyb 2 1` etc. We need `Nmesh+1` points where the endpoints $\tau = 0, \beta$ are included! By convention has negative sign. The local orbital levels are assumed to be $\tilde{\mu} = 0$ and any shift is absorbed in the chemical potential! This has to be checked for consistency!!!

**omega_mesh.dat** Specifies the bosonic frequency grid for some correlation functions. Just reuse the standard template file. Not important for us.

**fort.10*** Includes information about the Monte-Carlo configuration used for starting the sampling. Is initialized once with Yusuke's code and then overwritten by the solver. No change required here.

## 16.2 Bandstructure calculation

All data in the GW+DMFT calculation is given on the imaginary Matsubara frequency axis. To obtain the Bandstructure on real frequencies, we proceed as follows:

1. First, we create the Green's function for a given $k$-point on the Matsubara axis via

$$G(k, i\omega_n) = \big[\mathbb{1}(i\omega_n + \mu) - H^{DFT}(k) + v^{XC}(k) - \Sigma^{GW}(k, i\omega_n) + \Sigma^{GW,loc}(i\omega_n) - \Sigma^{imp}(i\omega_n)\big]^{-1} \tag{16.1}$$

   Or, for example, to obtain only the GW Bandstructure we set the impurity contributions to zero

$$G(k, i\omega_n) = \big[\mathbb{1}(i\omega_n + \mu) - H^{DFT}(k) + v^{XC}(k) - \Sigma^{GW}(k, i\omega_n)\big]^{-1} \tag{16.2}$$

   Then the Pade-approximation is applied to $G(k, i\omega_n)$ to obtain $G(k, \omega)$ on the real axis. This is done for all k-points. The spectral function is then given by

$$A(k, \omega) = -\frac{1}{\pi}\mathrm{Im}G(k, \omega) \tag{16.3}$$